# 25MM GUN DEMONSTRATION OF NITROGEN –DOPED BORON PROPELLANTS

Thelma Manning*, Michael Fair*, Nathan Peabody*, Viral Panchal*, Eugene Rozumov*, James Barnes**, Todd Cloutier**, Paul Matter***, Mary Powell***, Christopher Holt***

US Army DEVCOM Armaments Center *
Picatinny Arsenal, NJ 07806-5000
Veritay, Inc. 4845 Millersport Highway
East Amherst, NY 14051**
P H Matter
1275 Kinnear Rd., Columbus, OH 43212 ***

## ABSTRACT

The U.S. Army has a need for more powerful propellants with a balanced/stoichiometric ratio of fuel and oxidant to provide an advantage to its Warfighters. In addition to improved power, balanced propellants have reduced blast force and secondary flash, an important advantage in terms of signature for Soldiers. However, balanced propellants lead to accelerated wear and erosion of gun barrels due to the higher flame temperature. Ceramic additives in the propellant can theoretically prevent gun barrel deterioration by coating the barrel interior. Implementation of composite propellants with conventional ceramics (i.e., alumina) has not resulted in improved wear and erosion resistance to date. Due to challenges with dispersing the particles in the propellant, as well as incomplete sublimation, propellant and ceramic composites that produce regenerative wear-resistant coatings have not been effectively demonstrated. Boron nitride (in the form of crystalline hexagonal boron nitride or amorphous boron nitride) has the ideal properties of a propellant additive. Boron nitride can form a lubricating coating on gun barrel walls. Further, boron can dope steel, which drastically improves its strength and wear resistance. However, to form a thin coating that reduces abrasion, boron nitride must be in the form of a nano-particle, and must be evenly dispersed in the propellant. Further, the production of nano-scale boron nitride must be economical for implementation in advanced propellant composites. These materials can be dispersed in propellants to form a stable composite.

In this work, the technology will be demonstrated in a gun test stand. A successful demonstration will allow the technology to be transitioned to full scale gun demonstrations in the 155mm artillery M232/M232A1 propelling charge. The M232/M232A1 propelling charge consists of M31A2 triple base propellant containing nitrate ester plasticized nitrocellulose. The currently fielded 155mm artillery propelling charge, M232/M232A1, has exhibited spiral wear and erosion problems. This phenomenon has been attributed to a number of factors, such as the wear reducing liner that contains titanium dioxide, talc and wax, and the interaction of the propellant combustion products on the projectile rotating band within the gun tube wall. Modeling and simulation studies performed by Benet Labs have determined that the reaction of titanium dioxide with the talc and wax produced a residue that was hard to remove. This product was an abrasive residue (number 80 ceramic grit) that built up in the gun barrel causing a spiral rifling imbalance and accelerated gun barrel erosion, which markedly shortened gun barrel life. Boron nitride is an interesting potential additive to propellants that could reduce gun wear effects in advanced propellants. It has the properties of providing metal coating/lubricating, and steel hardening properties and nitrogen cooling. During propellant 25mm gun firing, the additive will either form hexagonal boron nitride, which can provide a protective coating and lubricating barrier on the inside of the barrel walls or oxidize to form boron oxide. Boron oxide could also coat the barrel or dope the steel with boron. Additionally, because of its low molecular weight, boron nitride oxidation could help to lower the propellant flame temperature. For this work, two different types of erosion steel sleeves will be fabricated to enable testing of propellant samples (baseline and three additive levels for each propellant).

In this paper, results from the 25mm ballistics gun firing of triple base propellant with boron nitride nano-composite propellants will be presented. This presentation will include vacuum thermal stability, closed bomb testing, and 25mm wear and erosion gun testing. Detailed characterization of the boron nitride incorporated into

gun propellant formulations, before and after 25mm firing, will be shown by methods including electron microscopy and x-ray photoelectron spectroscopy. Analysis of the post-mortem samples will also be presented. This promising boron nitride additive shows the ability to improve wear and erosion resistance, without any destabilizing affects to the propellant. Potential applications could include longer barrel life for large diameter firearms, and rocket propellants with reduced nozzle erosion rates.

## INTRODUCTION

The currently fielded 155mm artillery propelling charge, M232/M232A1, has exhibited spiral wear and erosion problems [1-8]. This phenomenon has been attributed to a number of factors such as the wear reducing liner that contains Titanium Dioxide, Talc and wax. Also the interaction of the propellant combustion products on the projectile rotating band within the gun tube wall. Modeling & Simulation studies performed from Benet Labs has determined that the reaction of Titanium Dioxide with the Talc and wax produced a residue that was hard to remove [1-3]. This product was an abrasive residue (number 80 ceramic grit) that built up in the gun barrel causing a spiral rifling imbalance and accelerated gun barrel erosion which markedly shortened gun barrel life. Boron nitride is an interesting potential additive to propellants that could reduce gun wear effects in advanced propellants [7,10-14]. It has the properties of providing metal coating/lubricating, and steel hardening properties and nitrogen cooling. During 25mm ballistics gun firing propellant, the additive will either form hexagonal boron nitride, which can provide a protective coating and lubricating barrier on the inside of the barrel walls, or oxidize to form boron oxide. Boron oxide could also coat the barrel, or dope the steel with boron. Additionally, because of its low molecular weight, boron nitride oxidation could help to lower the propellant flame temperature [3]. For this testing, erosion test steel sleeves will be used to enable testing of the propellant samples (baseline and three additive levels for each propellant) with two different types of erosion sleeves were fabricated.

## RESULTS AND DISCUSSION

In previous work on this project, a process was developed to prepare optimal BN additives for propellants. These materials can be dispersed in propellants to form a stable composite. Figure 1 below shows the concept for how the BN additive could provide a regenerative protective coating that could also harden the barrel.


**Figure 1**. Concept diagram showing how the propellant additive will provide a regenerative BN coating and hardening of the steel, resulting in decreased wear and erosion.

Previous wear and erosion testing (using propellant formulation RPD-380 with high flame temperature and high levels of nitrocellulose) has demonstrated the technology provides a 2-3X reduction in wear and erosion. The results are shown in Figure 2, achieving TRL of 5.

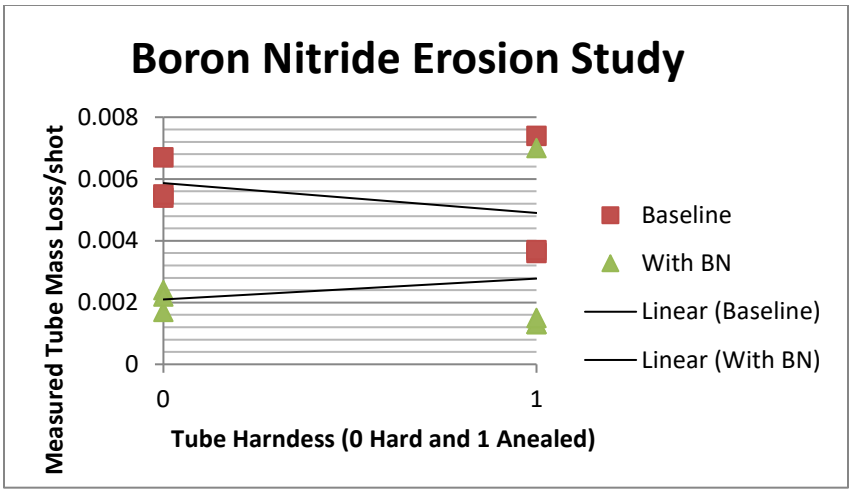


Figure 2. Phase II base period demonstration of 2-3X reduction in wear and erosion.

The SEM images of these NC based propellant samples fired in the erosion test stand and then cleaned are shown below in Figures 3a-3f. The steel showed a number of surface cracks. But the crack density appeared to be less, or were filled in, for the samples fired in boron nitride. The surfaces also appeared to be smoother and less pitted for the samples fired with boron. Figures 3a and 3b compare the hardened steel surface fired with and without boron nitride respectively. There appears to be more numerous smaller cracks in the samples fired without boron, in addition to a rougher surface. The differences are more apparent in the unhardened samples as seen in Figure 3c and 3d. The samples fired with boron nitride had fewer cracks, and/or the cracks were filled in. The surfaces appear smoother and more uniform for the samples fired with boron nitride. This is evident when magnifying to 10,000X, as shown in Figures 3e and 3f for the standard and BN composite samples, respectively. It is not clear from this characterization, if a $BN_xO_y$ product is coating the surface and/or filling in the cracks, or if boron dopes the steel, thus making it stronger and less likely to crack. Further characterization is required to understand these differences. If boron is doping the steel, one would expect it to increase the hardness of the steel.

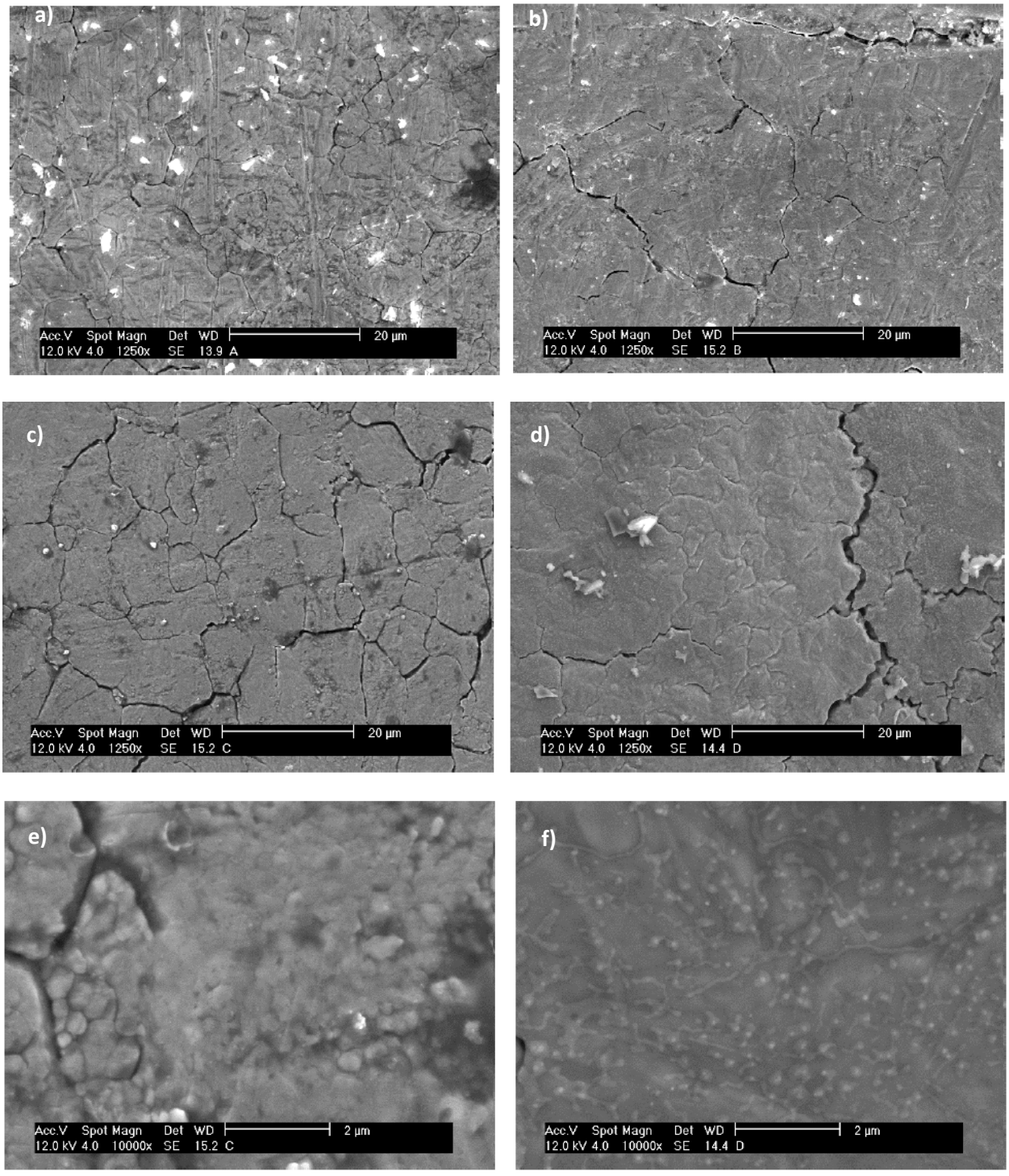


**Figure 3:** SEM surface images of: hardened steel inserts at 1,250 X magnification fired (a) in standard RPD-380, and (b) with BN / RPD-380 composite; unhardened steel insets at 1,250 X magnification fired (c) in standard RPD-380, and (d) with BN / RPD-380 composite; unhardened steel insets at 10,000 X magnification fired (e) in standard RPD-380, and (f) with BN / RPD-380 composite.

The primary objective of the project is to achieve TRL 6 for the BN additive technology through demonstrations in sub-scale gun testing. In previous months of the Enhancement phase of the project, a second batch of BN to DEVCOM AC, and steel selection (4330V alloy) were obtained. Veritay's 25-mm apparatus was unanimously agreed upon. DEVCOM AC prepared propellant formulations and delivered them to Veritay for testing.

PREPARATION OF BORON NITRIDE(BN)

In this subtask, PH Matter prepared BN materials for testing in propellants at DEVCOM-AC. In an effort to reduce production costs by 5X, PH Matter defined two new specifications for testing in the enhancement. Both specifications BN-A and BN-B were examined and down-selected for the second round of testing. The chemical properties of the BN have not changed from previous tested materials as shown in table 1, only the morphology

**Table 1.** Specifications for BN additive options

| Specification | Phase II BN | BN-A | BN-B |
|---|---|---|---|
| B:N Ratio | 1:1 +/- 0.05 | 1:1 +/- 0.05 | 1:1 +/- 0.05 |
| Oxygen Content | <10% | <10% | <10% |
| Surface Area | >20 $m^2/g$ | >20 $m^2/g$ | >20 $m^2/g$ |
| Morphology | >50% spheres | 5-25% spheres | 25-50% spheres |
| Metal Composition | None (ICP or AAS) | None (ICP or AAS) | None (ICP or AAS) |

PH Matter prepared and delivered BN-A and BN-B to DEVCOM AC for propellant preparation. Both materials were analyzed by X-ray Photo-electron Spectroscopy (XPS) and Inductively Coupled Plasma Atomic Emission Spectroscopy (ICP-AES). Figures 4a and 4b below show the XPS analysis of the BN-A and BN-B materials. Both had normal spectra for the B 1s and N 1s regions. The B:N ratio was 0.96:1 and 0.98:1, respectively, and no oxygen was detected in either sample, thus the materials passed the specifications. ICP confirmed that the materials were free of any potentially catalytic metals. The surface area was 51.7 $m^2/g$ and 65.9 $m^2/g$ for BN-A and BN-B, respectively.

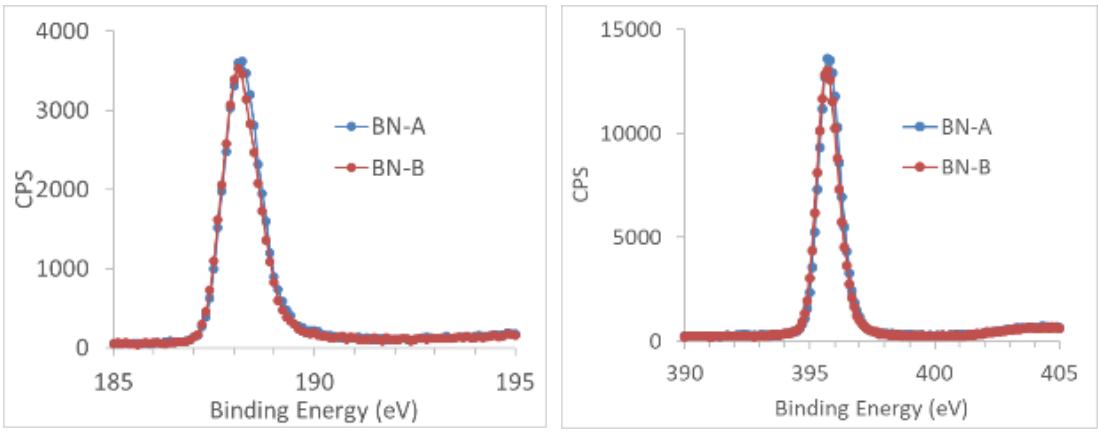


**Figure 4.** (a) the B 1s spectra region for the BN samples delivered to ARDEC, and (b) the N 1s spectra region for the BN samples delivered to ARDEC; the XPS analysis shows the materials are hexagonal boron nitride with the expected B:N ratios and less than 10% oxidation (no oxidation was detected).

PH Matter has prepared and delivered additional quantities of BN for propellant synthesis at DEVCOM AC.

COMPATIBILITY TESTS IAW STANAG 4147

Compatibility tests were conducted before the manufacture of the M31A2 propellant mixes following processing safety protocols.

Using a Differential Scanning Calorimeter (DSC), M31A2 propellant constituents were run through a temperature scan as controls. These test were run in duplicate, the M31A2 propellant in combination with the M31A2 formulation constituents IAW STANAG 4147. The recorded from the DSC is essentially a thermal profile. The profile included a melting point, an ignition / decomposition temperature or both, depending on the nature of the energetic as shown in Figures 5a, b, c, and d.

The M31A2 propellant control sample shown in Figures 4a and 4b, respectively, displayed an average peak temperature of 186.53 degrees Celsius.

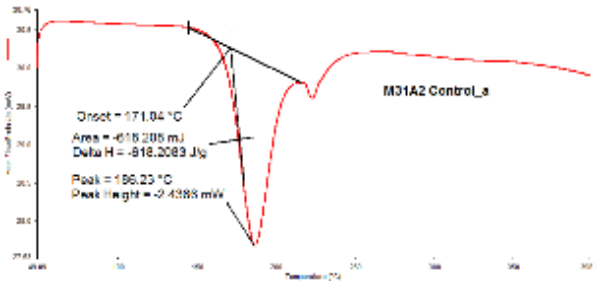


Figure 5a. DSC scan for the M31A2 propellant as Control a.

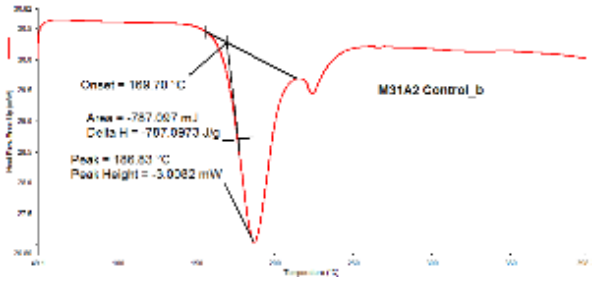


Figure 5b. DSC scan for the M31A2 propellant as Control b.

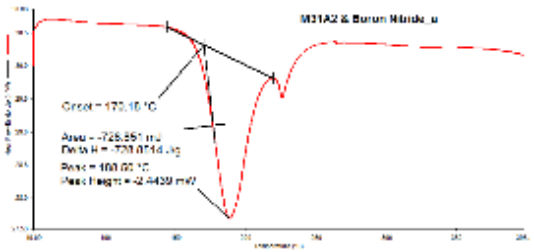

Figure 5c. DSC scan for the M31A2 propellant with BN.

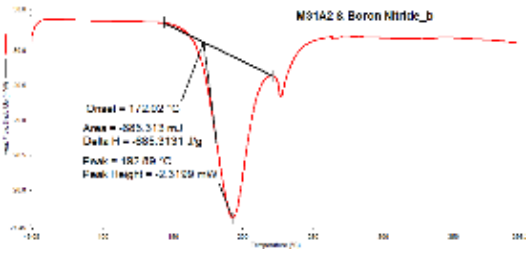

Figure 5d. DSC scan for the M31A2 propellant with BN

| Samples | Peak Temp (°C) | Criteria | Result |
|---|---|---|---|
| | | | |
| M31A2 Control a | 186.23 | | |
| M31A2 Control a | 186.83 | | |
| M31A2/Boron Nitride_a | 188.5 | within or greater than 4 degrees shift to the right of M31A2 control | pass |
| M31A2/Boron Nitride_b | 192.86 | within or greater than 4 degrees shift to the right of M31A2 control | pass |
| M31A2/Titanium Dioxide_a | 192.14 | within or greater than 4 degrees shift to the right of M31A2 control | pass |
| M31A2/Titanium Dioxide_b | 188.64 | within or greater than 4 degrees shift to the right of M31A2 control | pass |
| M31A2/Talc_a | 187.7 | within or greater than 4 degrees shift to the right of M31A2 control | pass |
| M31A2/Talc_b | 186.8 | within or greater than 4 degrees shift to the right of M31A2 control | pass |
| M31A2/Talc/Titanium Dioxide_a | 188.9 | within or greater than 4 degrees shift to the right of M31A2 control | pass |
| M31A2/Talc/Titanium Dioxide_b | 187.23 | within or greater than 4 degrees shift to the right of M31A2 control | pass |
| M31A2/Talc/Titanium Dioxide/Boron Nitride_a | 189.49 | within or greater than 4 degrees shift to the right of M31A2 control | pass |
| M31A2/Talc/Titanium Dioxide/Boron Nitride_b | 190.15 | within or greater than 4 degrees shift to the right of M31A2 control | pass |
| M31A2/Talc/Boron Nitride_a | 189.2 | within or greater than 4 degrees shift to the right of M31A2 control | pass |
| M31A2/Talc/Boron Nitride_b | 190.3 | within or greater than 4 degrees shift to the right of M31A2 control | pass |
| M31A2/Titanium Dioxide/Boron Nitride_a | 190.1 | within or greater than 4 degrees shift to the right of M31A2 control | pass |
| M31A2/Titanium Dioxide/Boron Nitride_b | 190.45 | within or greater than 4 degrees shift to the right of M31A2 control | pass |

Table 2. Summary of Peak Temperatures of M31A2 propellant samples and constituents from DSC Tests.

Table 2 shows a listing of the M31A2 propellant constituents and the peak temperatures from DSC compatibility tests. A DSC decomposition peak temperature shift of 4 degrees Celsius or less is deemed compatible. Any shift towards a lower peak temperature of the explosive has some degree of incompatibility. The greater the shift towards lower temperatures; the greater the degree of incompatibility will be. A peak temperature shift of more than 20 degrees indicates incompatibility. A degree shift of more than 4 degrees Celsius to the right is also deemed compatible.

Based on test results shown in Table 2, which were conducted in accordance with the defining criteria of IAW STANAG 4147 NATO/ U.S. military specifications (Chemical Compatibility of Ammunition Components with Explosives), M31A2 is deemed compatible when tested with Boron Nitride, Titanium Dioxide, and Talc combinations utilizing DSC thermal procedures.

## MANUFACTURE OF M31A2 PROPELLANTS AT DEVCOM AC FACILITY

DEVCOM AC completed propellant preparation and delivery of 8 lots of propellant listed in Table 3 and 450 M793 TP-T projectiles. The shipment of 442 Primed 25mm Cases (primed without propellant) were also completed.

| CONSTITUENT | PN RDD20A-00381-A1 graphite coated and undeterred | PN RDD20A-00381-A2 graphite coated and deterred | PN RDD20A-00382-A1 graphite coated and undeterred | PN RDD21A-00382-A2 graphite coated and deterred | PN RDD21A-00385-A1 graphite coated and undeterred | PN RDD21A-00385-A2 graphite coated and deterred | PN RDD21A-00387-A1 graphite coated and undeterred | PN RDD21A-00387-A2 graphite coated and deterred |
|---|---|---|---|---|---|---|---|---|

Table 3. Manufactured of 8 lots of M31A2 propellant processed at DEVCOM facility.

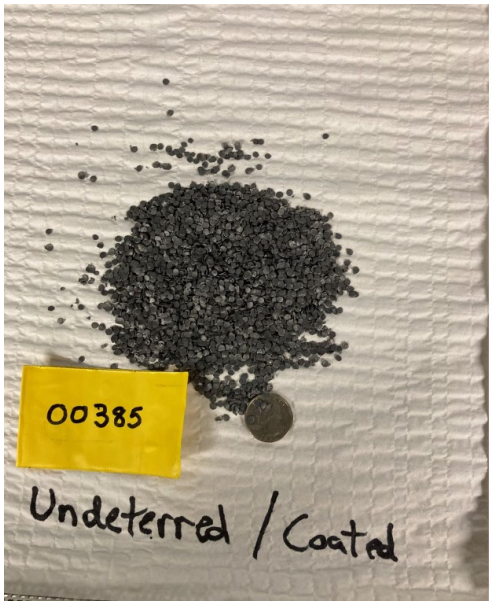


Figure 6a: Lot # RDD21A-00385-A1
Graphite Coated and Undeterred


Figure 6b: Lot # RDD21A-00385-A2
Graphite Coated and Deterred

Four base propellant formulations lots shown in table 3 were produced at DEVCOM facility, and a portion of each lot was deterred to assist in developing a propellant charge that will produce acceptable ballistics as shown in Figures 6a and 6b. The propellant grain geometry shown in Figures 6a and 6b were extruded into 0.141-inch diameter and 0.0186 inch in length.

## FIRING TESTING USING A 25MM EROSION TEST FIXTURE

To evaluate the ability of nanomaterial propellant additives to increase the effective barrel lifetime of gun tubes, gun firing tests using the propellant formulations produced will be carried out at Veritay Facility. Veritay will make use of a 25 mm Erosion Test Fixture (ETF). This fixture utilizes a replaceable barrel section near the origin of rifling. This barrel section will precisely measure both before and after testing to ascertain the degree of erosion associated with each of the propellant formulations tested. A total of three (3) propellant formulations, baseline without any additive, two with various combination of the charge constituents attributed to causing the residue and with varying levels of additive will be sent to Veritay for gun testing. For each of these M31A2 modified formulations, twenty-five (25) lbs. of

propellant were manufactured by DEVCOM AC, half was deterred with a deterrent such as Ethyl Centralite (at a level of at 2-3%) and half undeterred.

All of the ammunition components were provided to Veritay as Government Furnished Material (GFM). This includes, in addition to the propellant, primed 25mm cartridge cases (with flashtube and booster as appropriate), and M793TP projectiles.

Veritay set up a 25mm test fixture and determine ballistics for the 25mm round using the baseline M31A2 propellant formulation, with different combinations of charge constituents and propellant with various levels of the additive. For each of the propellant formulations, Veritay adjusted the deterred and undeterred propellant charge masses until the appropriate pressure and velocity are achieved. The M793TP rounds will be cut down to adjust the mass of the projectile to one more suitable to a high velocity round (around 120 g). The actual mass will also be determined during this task.

For this testing in the ETF, Veritay will fabricate erosion test sleeves to enable testing of the propellant samples with an erosion sleeve that represents a steel artillery cannon. All three of the propellant samples will be tested with these erosion sleeves, up to thirty shots per sleeve. This comprehensive approach that will ensure that usable comparisons of the erosivity/residue of the various propellant samples can be achieved. The un-chromed steel sleeves are more prone to surface gun barrel erosion, allowing a comparison to be measured.

An associated Joint Army NASA Navy Air Force (JANNAF) paper by S. Sopok “Charge-Additive Induced Gun-Bore Residue Deposition Model”, addresses recent 155mm bore deposits that cannot be cleaned in field, are difficult to clean at Proving Ground & can cause ammo loading problems, gun tube spiral wear & early fuse function. The paper discussed the development of a unique new 155mm gun bore residue deposition models for key charges/zones with additives to accurately predict if and clearly explain why the M232A1/5 bore deposits start farther up-bore than M232/5, M232A1/5 bore deposits thicker (0.020”/25 rounds) with bigger band than M232/5, the Top-zone charge bore deposits more than zone-four counterparts, the Up-bore deposits can enable spiral wear, the bore deposits adhere & build-up on steel bore and on HC-Cr/steel bore. The results showed clearly show the root cause of “hard to clean” 155mm bore residue deposit that cannot be cleaned in field/difficult at Proving Ground, deposit formation, onset location, magnitude & band length that can enable spiral wear, ammo loading problems & early fuse function [1].

Additionally, an associated Joint Army NASA Navy Air Force (JANNAF) paper by S. Sopok, Gun Bore Deposit Model For Single Wear Additive Charges”, recently developed 155mm fielded gun-bore deposition models to further develop modified M232A1 and M232 charge models with single wear additives to accurately predict if and clearly explain why modified M232A1/5, M232/5, M232A1/4 & M232/4 charges each with TiO2 produce minimal bore-brush-cleanable deposits vs “hard to clean” fielded counterparts, modified M232A1/5, M232/5, M232A1/4 and M232/4 charges each without talc produce minimal bore-brush-cleanable deposits vs “hard to clean” fielded counterparts and modified charges without talc produce less bore-brush-cleanable deposits than modified charges w/o TiO2. The paper discusses the root cause of “hard to clean” fielded dual-wear-additive-charge bore deposits, root cause of predicted bore-brush-cleanable modified single-wear-additive-charge bore-deposits (TiO2, talc), deposit formation, onset location, magnitude & band length for four charge-zone combinations [2].

A method, AIN 024-16A, has been developed by the artillery office in describing residue by recording distance from the rear face of tube (RFT) and describing the residue category observed in the hardened down-bore cannon when firing 155mm howitzers with the M203A1 and M232A1 charges.

All materials required to start testing have been received at Veritay; this includes the AISI 4330V erosion rings, primed cartridge cases, M793 TP-T projectiles, and the modified M31A2 propellant listed in Table 3. Four base propellant formulations lots were produced at DEVCOM facility, and a portion of each lot was deterred to assist in developing a prop charge that will produce acceptable ballistics shown in Figures 5a and 5b.

The first task upon receipt of the propellant by Veritay was to determine the proper propellant charge mass. Each propellant was provided in two versions, undeterred (A1) and deterred (A2). A limited number of extrusion dies were available to the project, which in turn, limited the propellant form function that could be produced. The 25mm round typically uses a 7-perf propellant grain, however the Army was not able to produce that with the available dies. After discussions with the stakeholders, it was agreed that the Army would produce a flake propellant using the smallest die, with a web that would produce acceptable ballistics in the 25mm gun. The following grain dimensions were determined using IBHVG2 with a charge mass of 70 grams and a projectile mass of 140 grams and a target pressure of 55,000 psi. A ballistic workup was performed for each propellant in an instrumented 25mm man barrel. The cartridges were drilled to measure chamber pressure and velocity was obtained through break strips. Charge mass was limited to 65 – 66 grams of propellant, owing to the lower bulk (settling) density of the flake propellant grain compared to that of a 7-perf cylindrical grain. This prevented our ability to load the cartridges to the loading density that was assumed for the IBHVG2 calculations, which resulted in a lower chamber pressure than predicted. The reduction in chamber pressure was partially mitigated by the M793T-PT projectiles, which are 40 grams heavier than the projectile mass used in the IBHVG2 model. The muzzle velocity generated is reasonable surrogate for a howitzer (around 3000fps). All shots used only the undeterred propellant variant. The resulting peak chamber pressure and velocity are shown in the following table. Pressure vs. time curves for all four propellants are shown in Figure 7. All of the propellants were well behaved with no ignition issues or pressure anomalies.

As mentioned above, despite the chamber pressure and velocity, being lower than predicted in the IBHVG2 models, they are within the range of what would be experienced in a Howitzer gun system. Given the time constraints of this program, testing proceeded with the maximum propellant loading. Consequently, Veritay prepared 30 cartridges of each propellant variant for test firing in the 25-mm ETF.

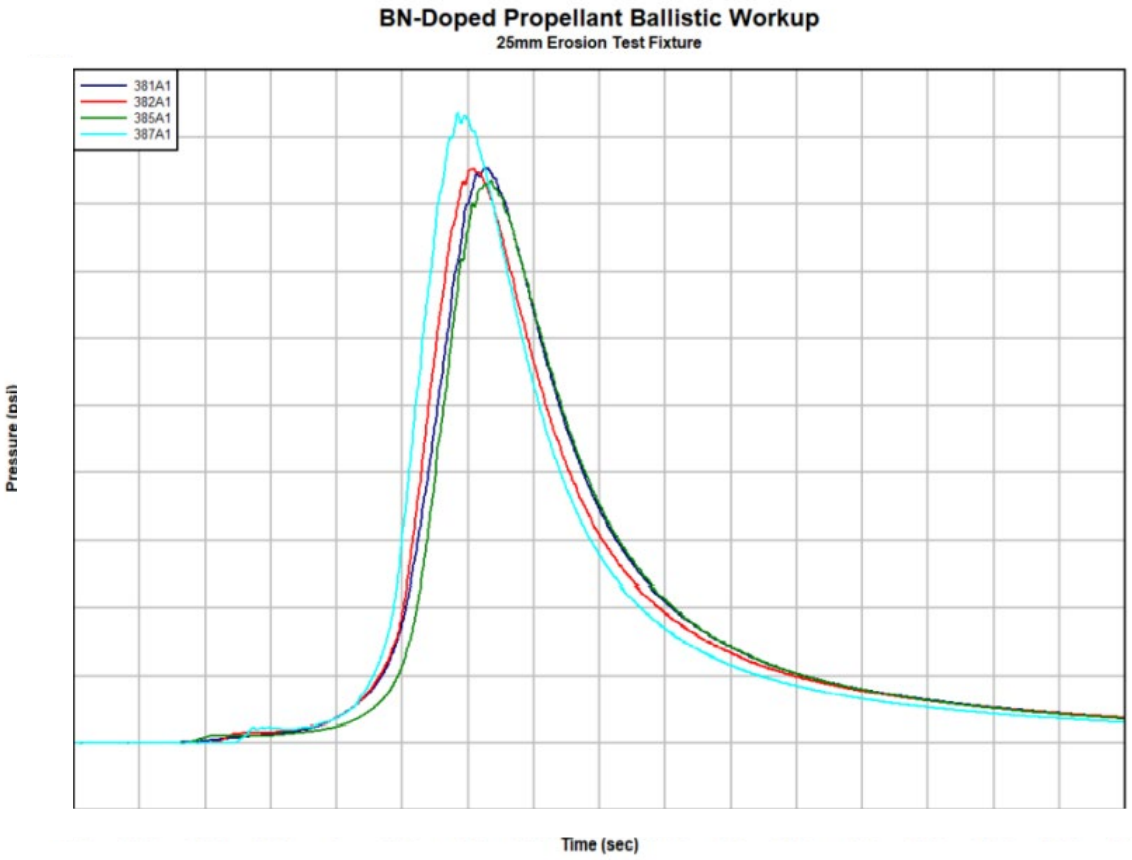


**Figure 7.** BN-doped propellant ballistic measurements.

Initial measurements of the 25 mm erosion rings were completed prior to testing. The measurements were performed on a Helmet Coordinate Measuring Machine (CMM) at ten locations on each rifling land and groove, starting at 0.1 inches from the end of the ring furthest from the chamber and at axial increments of 0.1 inches. A sample of the measurement report summary is shown in the Figure 8. In the summary report, a circle was fit to the individual measurement points to arrive at a diameter for each of the ten measurement depths, noted as DIA in the tabulated data. The tabulated data in the summary reports shows the nominal diameter (NOM) from the CAD model, the actual diameter (ACT) from the CMM measurement, and the deviation from nominal (DEV). A spreadsheet with the individual measurement point coordinates was also produced. In addition, fifty (50) rounds of each of the propellant formulations were loaded in the 25mm cartridges for use in test firing the four erosion rings. Once this was complete, test firings were performed. Fifty shots were fired on each erosion ring, using the propellant charge weights discussed above and in last month's report. After firing, the exterior surfaces of the erosion ring were cleaned. The bore surface was wiped with a paper towel, but otherwise was not mechanically or chemically cleaned. Photos of each erosion ring are shown in Figures 9 through 12. A light gray residue was present on the bore surface, but there did not appear to be a significant accumulation.

For reference, a close-up image of the insert surface is shown in Figure 13 for an unfired insert. The landings displayed horizontal markings consistent with machining.

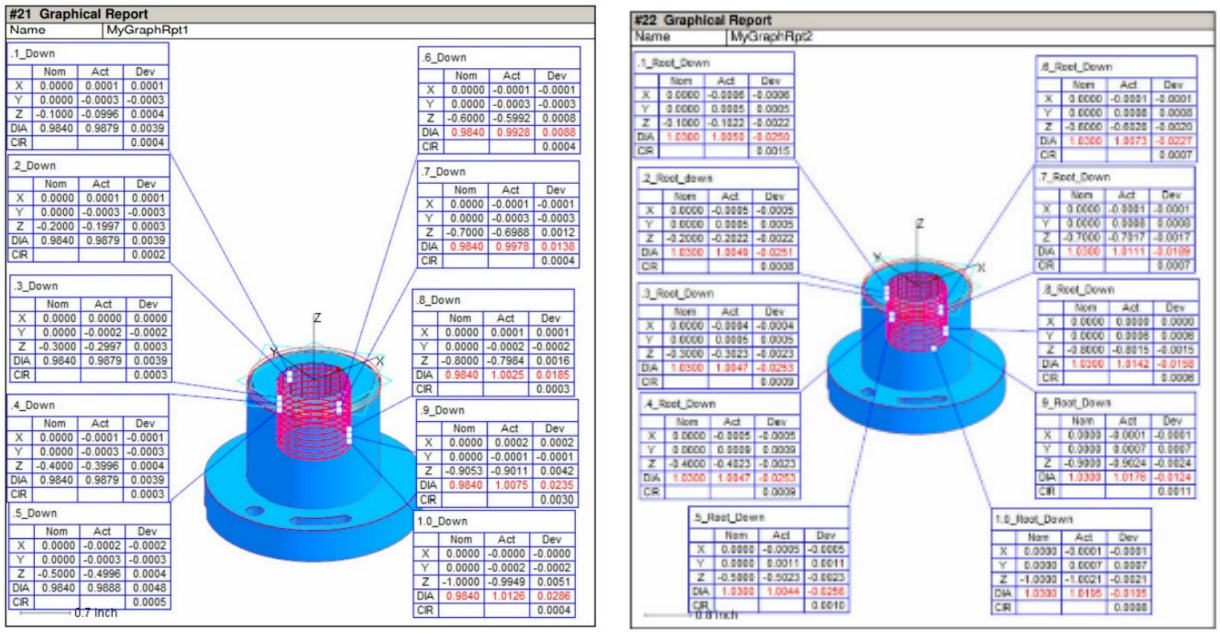


**Figure 8.** Measurement reports for erosion ring rifling lands.

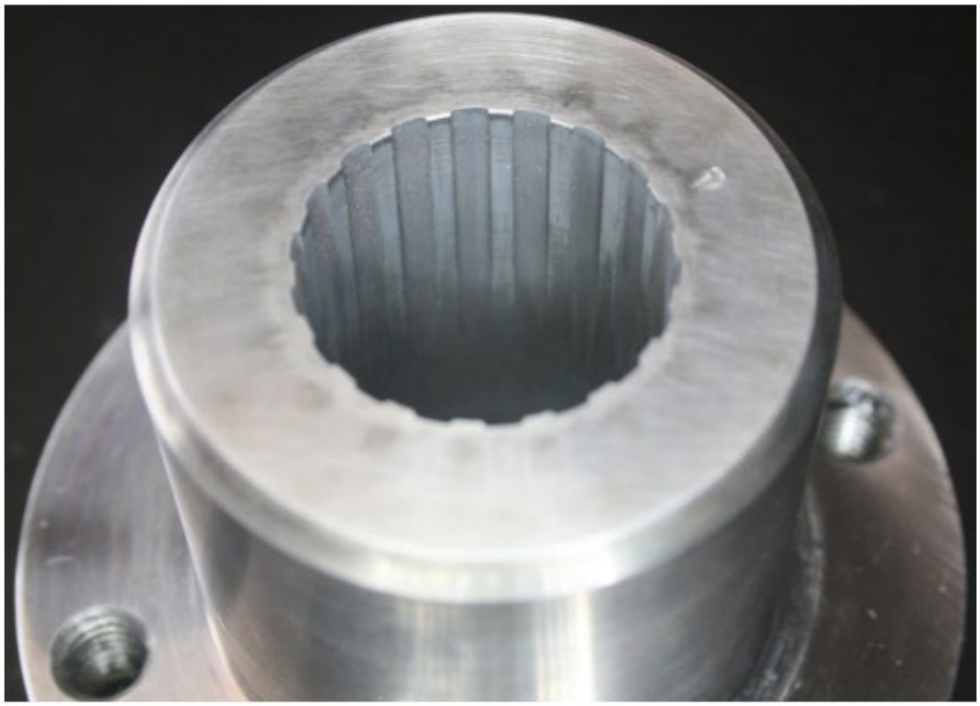

**Figure 9.** Erosion ring sample number 1 after firing 50 shots with propellant 381A1.

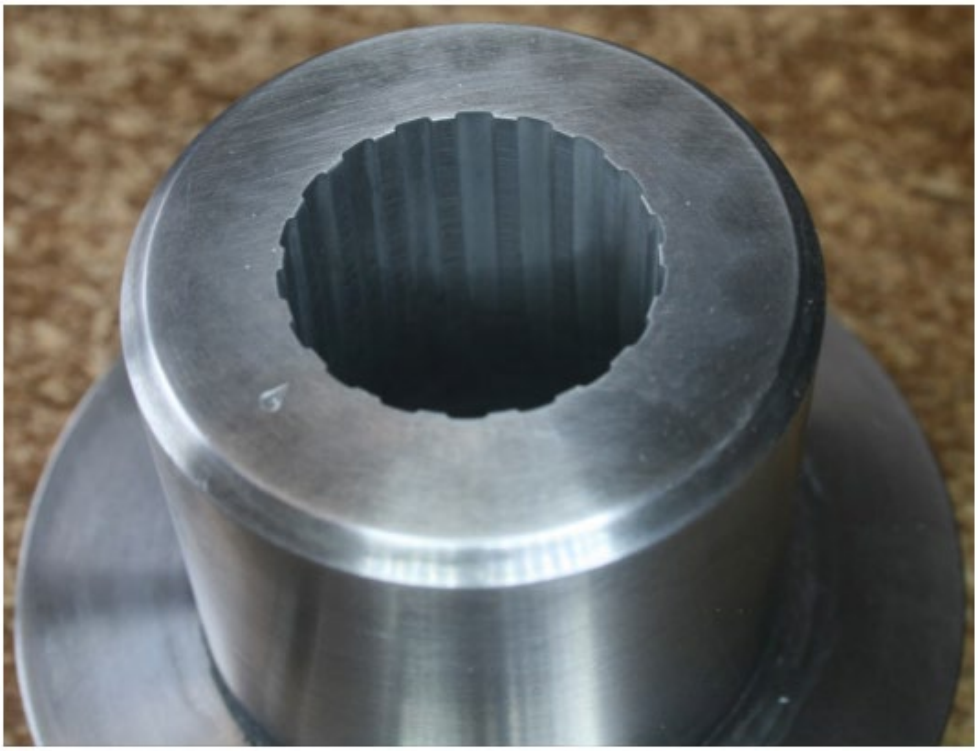

**Figure 10.** Erosion ring sample number 2 after firing 50 shots with propellant 382A1.

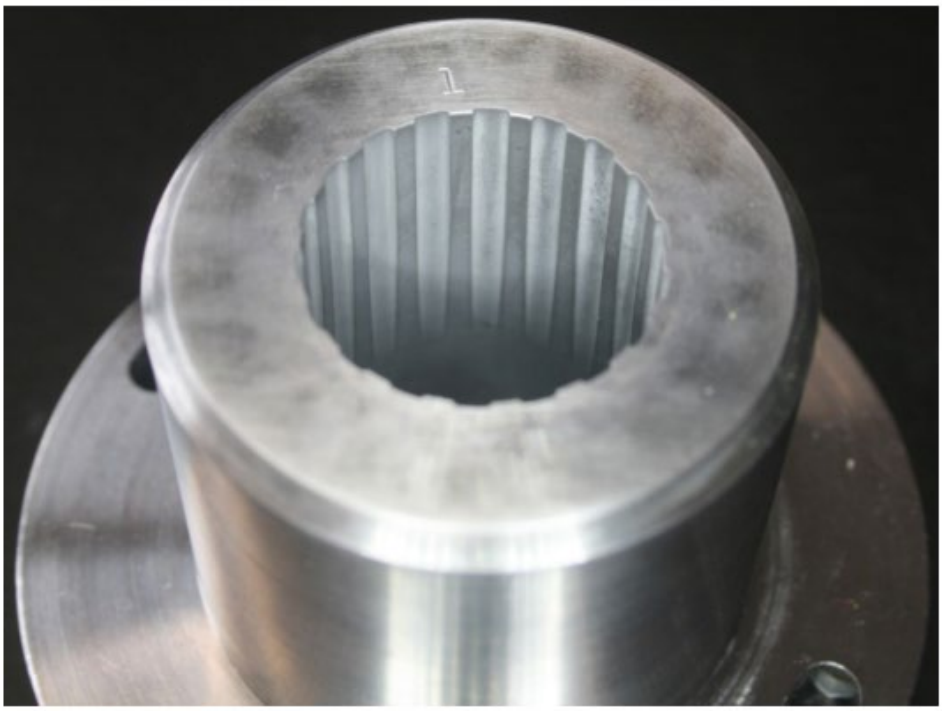

**Figure 11.** Erosion ring sample number 3 after firing 50 shots with propellant 385A1.

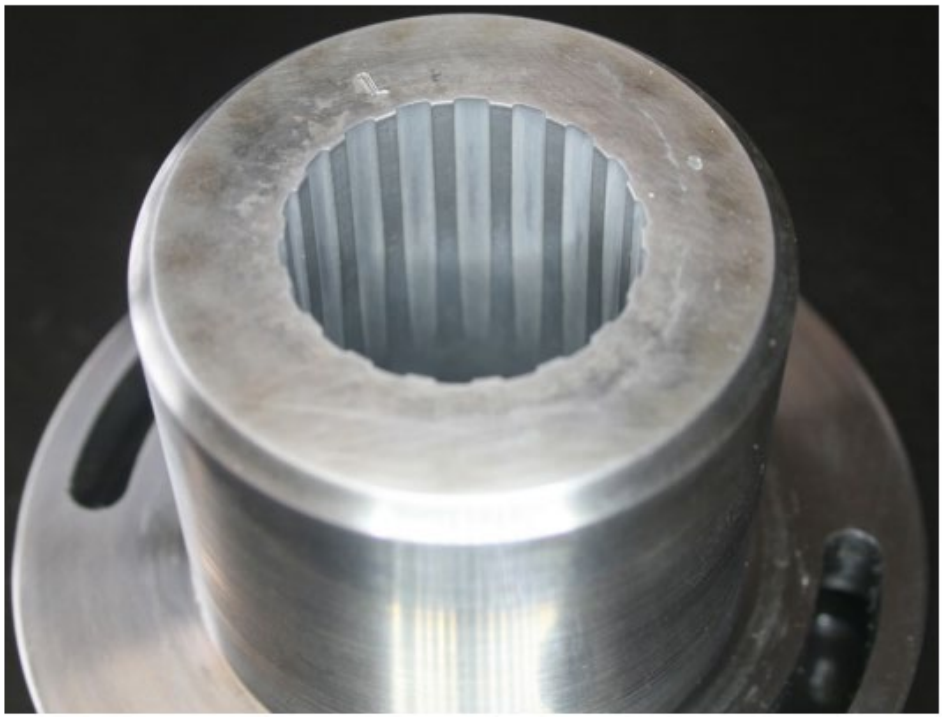

**Figure12.** Erosion ring number 4 after firing 50 shots with propellant 387A1.

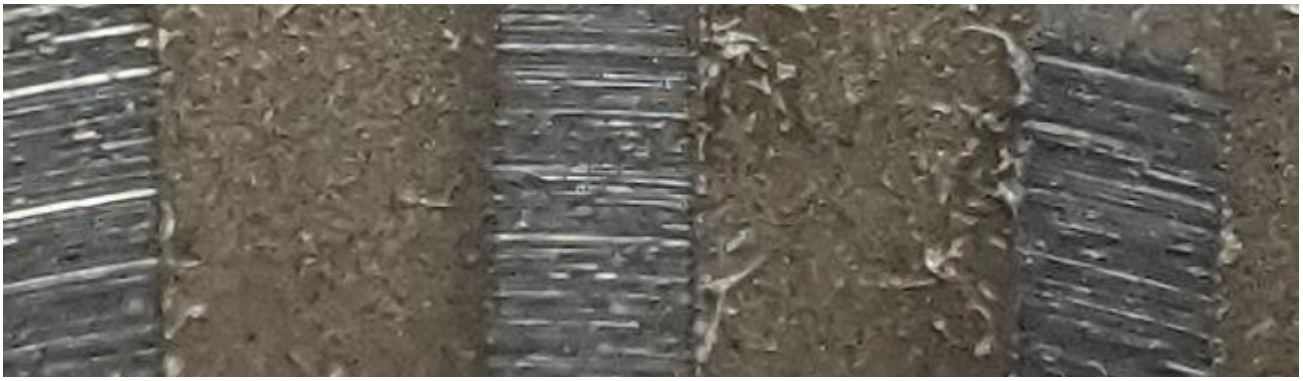

**Figure 13.** Photograph of an unfired insert showing grooves on the landings from machining.

The erosion rings were measured by an external Vendor, then returned to Veritay. Upon evaluation of the measurement results, there appeared to be an anomaly with ring #1 which had been tested with the baseline M31A2 propellant. Ring #1 showed nearly 0.020-inch of erosion on the diameter in the rifling grooves, much greater than anticipated given the low-erosion nature of M31A2 (relatively cool flame temperature), but little change on the lands. The anomaly seems to have occurred in the initial measurement of Ring #1, leading to the appearance of an excessive amount of erosion. The remaining rings showed little dimensional change, which conformed to our expectations going into the test program. The anomalous results for Ring #1 could be the result of an error in the measurement process, or a consequence of the rifling machining method. We have previously measured the erosion rings by hand, using a micrometer and a measurement fixture. This process is time consuming, and the results can be dependent upon the person performing the measurements. The use of a coordinate measurement machine (CMM) to automate the measurements was expected to expedite the

measurement process while improving repeatability by removing the human factor. However, we cannot ignore the possibility that an error occurred somewhere in the CMM process leading to the anomaly seen in the grooves of ring #1. It is also possible (although unlikely) that the anomalous results for ring #1 were a consequence of the machining method. The erosion ring rifling grooves were cut using wire electrical discharge machining (wire EDM) as opposed to a mechanical machining method (e.g., broaching). Industry literature indicates the possibility of re-deposition of removed material, or material from the EDM wire, onto the machined surface, dependent on the EDM machine settings. A chemically altered “white layer” is also formed on the machined surface by the wire EDM process, which may be a contributory factor. Examination of an unused erosion ring shows some discoloration of the EDM surface, which is no longer present in Ring #1 after firing. In order to eliminate the machining method as a variable in future erosion tests, the EDM surface should be media-blasted prior to surface treatments and measurement to remove the “white layer” and any deposited materials. For this to be a more likely occurrence, we would expect the 2 same effect on all four of the sample rings, not just on ring #1. Also, the magnitude of the anomaly (about 0.020”) contributes to the unlikelihood that it had something to do with redeposition of the EDM wire itself. As a result of the anomalous measurements of ring #1, we executed a second test series of 50 rounds on each of the four erosion rings and sent them out for re-measurement. The following two graphs show the change in groove and land diameter after the second test series of fifty shots with each propellant, compared to the measurements after the first 50 shots had been fired. Measurements were taken every 0.1-inch axially, starting at the muzzle end of the erosion ring, proceeding axially towards the chamber. A positive change in the diameter indicates erosion of the bore, while a negative change in the diameter is suggestive of the presence of residue.

The measurement results for the second test series showed minimal dimensional change to the diameters of both the rifling grooves and lands. The measurement repeatability was about ±0.1 thousandths of an inch (±2.54 μm). Although the change in bore diameter was minimal, there may be a trend of reduced erosion for the three propellants with the BN additive. In Figure 14, Ring #1 exhibits a groove diameter increase of 0.2 to 0.3 thousandths of an inch at the muzzle end of the erosion ring, while the remaining three rings show no erosion and potentially a small amount of residue. Ring #4, fired with the BN additive combination, exhibits the most potential residue at the muzzle end of the erosion ring, at least in the grooves.

The potential trend of the propellant additives reducing erosion continues for the rifling lands, shown in Figure 15. Ring #1 exhibits a diameter increase of 0.2 thousandths of an inch (5.08 μm) on the land diameter at the chamber end of the erosion ring. Rings #2 through #4 fall within the measurement uncertainty, with Ring #2 having some possible residue at the muzzle end.

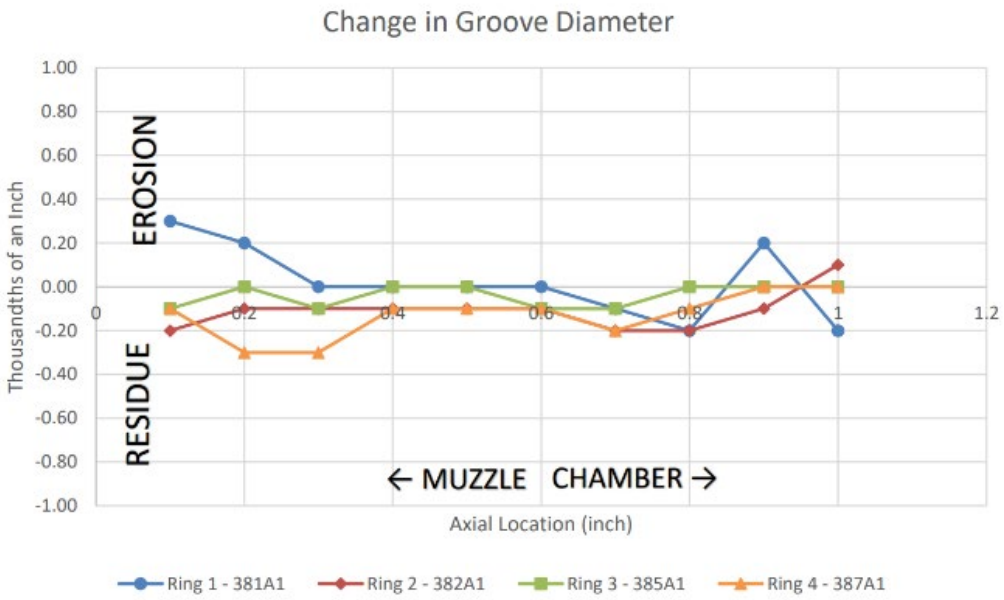


**Figure 14.** Change in rifling groove diameter after 50 shots (2nd test series)

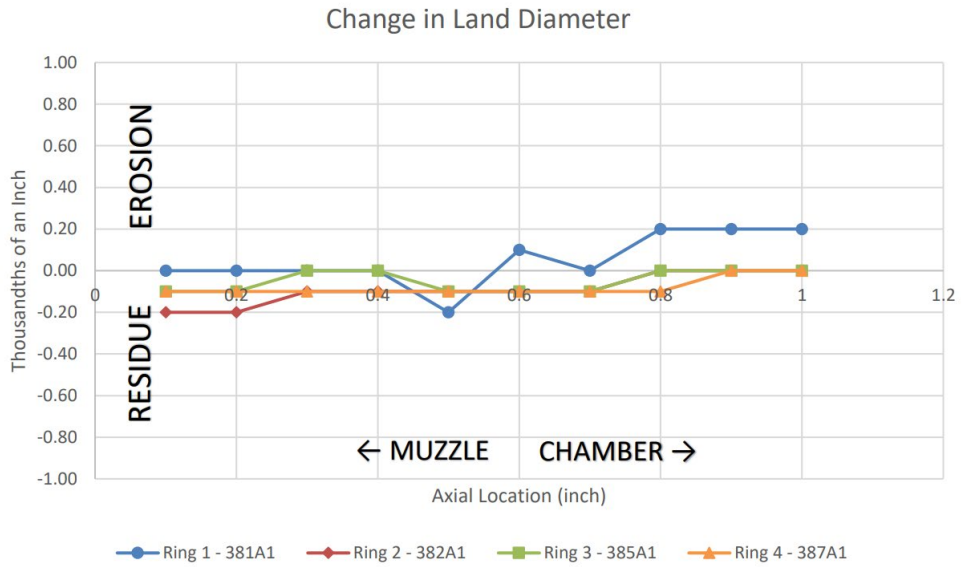


**Figure 15.** Change in land diameter after 50 shots (2nd test series).

It is difficult to draw definitive conclusions related to the efficacy of the propellant additives given the small dimensional changes produced by the modified M31A2 propellant. However, there is evidence that the additives have an effect when compared to the baseline propellant with no additives. While many of the measurements fall within the uncertainty of the measurement technique, overall trends do suggest an improvement was realized. As originally proposed, a hotter, more erosive propellant such as RPD380 or even JA2 would have produced a more definitive quantification of erosion and the potential effects to ameliorate this by the additives inserted into the mixes, in a more limited quantity of test shots fired. Veritay suggests the use of this approach for future efforts that may have an interest in similar additives and their effects on very erosive propellants.

After return of the inserts from the Vendor, they were delivered to pH Matter for further analysis.

## INSERT SAMPLES POSTMORTEM ANALYSIS

After firing, the insert samples were analyzed by using facilities at nearby Ohio State University. As described below, the analysis techniques include Scanning Electron Microscopy (SEM), X-ray Photo-electron Spectroscopy (XPS), Inductively Coupled Plasma Mass Spectrometry (ICP-MS) analysis, and Moh's hardness testing.

Samples for the analyses were taken from the same location of each insert, as shown in Figure 16 below. The muzzle end of each insert was cut off approximately 7.5 mm from the end. Next, slices with an individual ridge (or "lands") were cut from the sample ring. Each land was reduced to a 6 mm depth without disturbing the surface of the ridge / lands. Moh's hardness testing, SEM imaging, and XPS analysis was performed on the lands near the center (3-4 mm from the muzzle tip). ICP analysis was performed on the entire 6 mm x 6 mm x 7.5 mm lands sample.

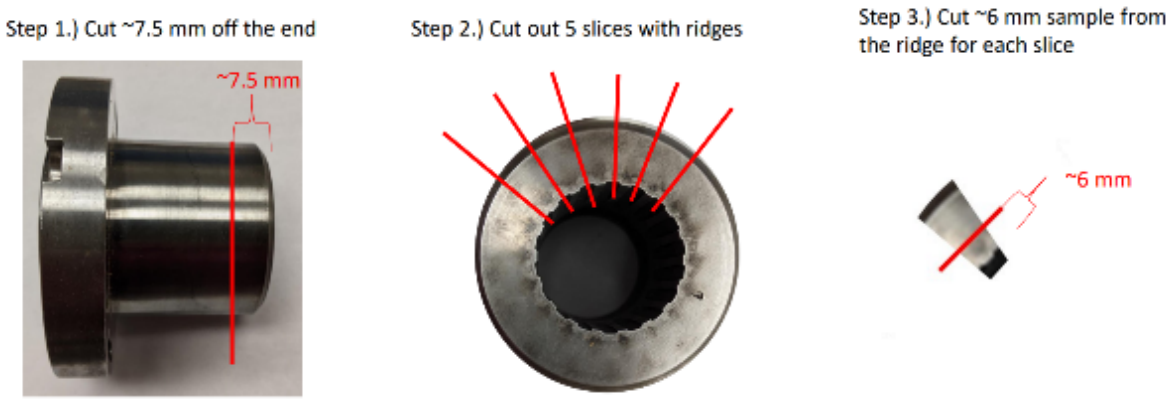


**Figure 16.** Instructions and location for sample analysis.

***Moh's Hardness Testing.*** Moh's hardness testing was performed using in-house hardware available at pH Matter. This technique measure hardness by determining what hardness of test tip can scratch the surface of a sample. All of the samples had residue that could be removed with a harness test tip of 4. However, the hardness 4 tip material could not visibly scratch the underlying metal for any sample. The metal surface of Sample #1 and #2 were visibly scratched by a hardness 5 tip. Samples #3 and #4 were resistant to scratching with the hardness 5 tip, and visible ridges, apparently from the machining process, were still apparent on the surface even after the hardness 5 tip test. With a hardness 6 tip test the ridges were visible scratched by the tester. Consequently, as shown in table 6, samples #1 and #2 have a hardness of between 4 and 5, while samples #3 and #4 have a hardness between 5 and 6. For reference, hardness of 4.5 is consistent with nickel, iron metal, stainless and ordinary steel. Hardened steel can be as high as 7 on the Moh's scale.

| | Sample #1 (381A1) | Sample #2 (382A1) | Sample #3 (385A1) | Sample #4 (387A1) |
|---|---|---|---|---|
| **Surface Hardness Measured** | 4.5 | 4.5 | 5.5 | 5.5 |

**Table 4.** Results from Moh's Hardness Testing.

***SEM Analysis***. SEM imaging with Energy Dispersive X-ray Analysis (EDAX) was used to observe the morphology of the lands surface and elemental analysis. Figures 17-20 below compares samples #1-4. Sample #1 had a smooth land surface that appeared to be predominantly iron on a mass basis. Samples 2, 3, and 4 all appeared to have ridges. These ridges appear to be consistent with machine marks on the land from the original turning of the parts (see photograph in Figure 13 above) – the finish on these parts were specified as 32 micro-inch roughness. Sample #3, which had the highest BN loading in the propellant, showed the most-defined ridges. This potentially indicates that the BN helps the steel maintain its finish roughness even after firing. Samples 2-4 had less iron exposed on the surface than Sample #1. Boron cannot be detected with SEM/EDAX analysis due to signal interference with carbon. The EDAX analysis depth is approximately **1-2 microns**.

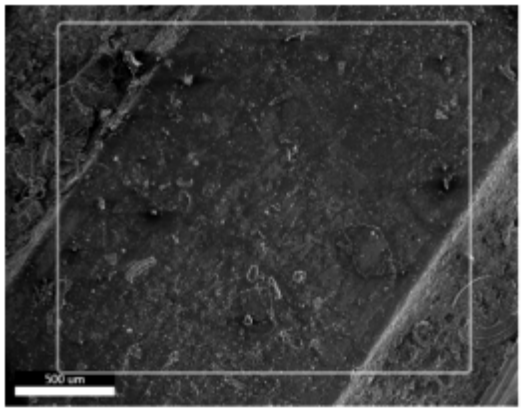


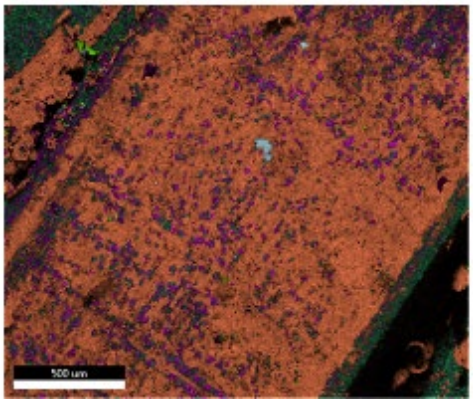


**Figure 17.** SEM analysis of sample #1 EDAX elemental analysis by mass of sample #1

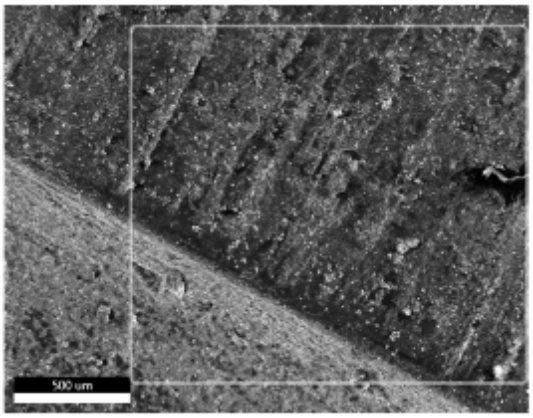


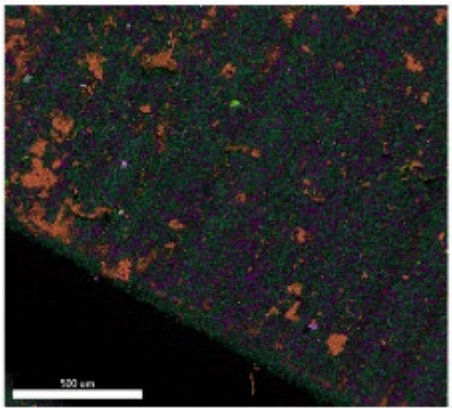


**Figure 18.** SEM analysis of sample #2 EDAX elemental analysis by mass of sample #2

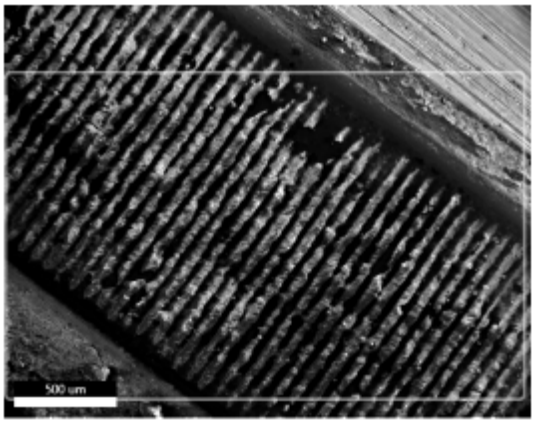


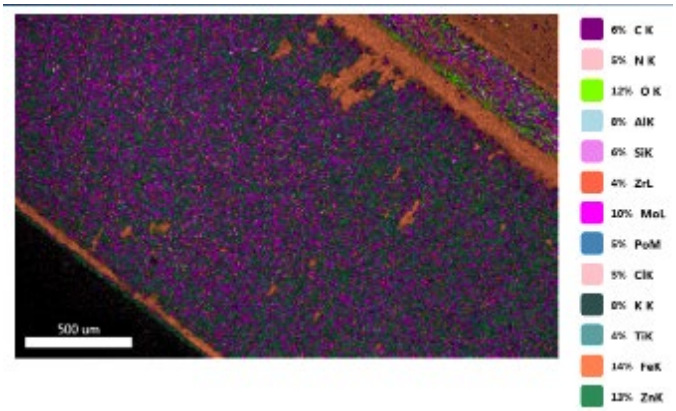


**Figure 19.** SEM analysis of sample #3 EDAX elemental analysis by mass of sample #3

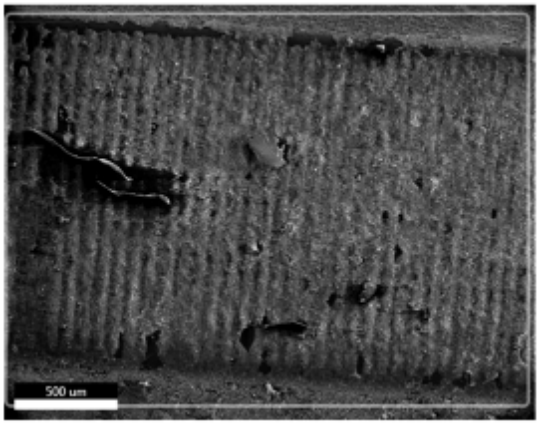


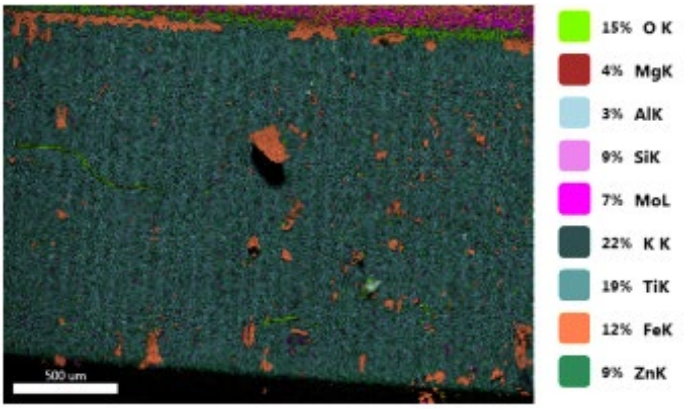


**Figure 20.** SEM analysis of sample #4 EDAX elemental analysis by mass of sample #4

***ICP-MS Analysis***. One theory for the improved hardness of boron fired samples is that the boron dopes the steel. ICP-MS analysis was performed by NSL Analytical to determine the boron content of the samples. Table 5 shows the results of ICP-MS analysis. Only Sample #3 contained a detectable amount of boron, measured to be 30 ppm. This happens to be the sample fired with the highest amount of BN in the propellant. However, it is possible the boron is from residue that was not fully removed during the barrel cleaning process. Also, although <10 ppm is a small amount of boron, boron can dope grain boundaries and harden steel in small quantities. Further, due to machining limitations, the samples were cut 6 mm deep. Doping is likely only required at the surface to increase steel hardness. Still, these results provide some indication of how much boron may be in the steel.

**Table 5.** Results of ICP-MS analysis of the insert boron content after firing.

| | Sample #1 (381A1) | Sample #2 (382A1) | Sample #3 (385A1) | Sample #4 (387A1) |
|---|---|---|---|---|

| | | | | |
|---|---|---|---|---|
| **B Content Measured** | <10 ppm | <10 ppm | 30 ppm | <10 ppm |

***XPS Analysis***. X-ray Photoelectron Spectroscopy (XPS), also known as Electron Spectroscopy for Chemical Analysis (ESCA), is used to determine semi-quantitative atomic composition and chemistry. XPS works by irradiating a sample with monochromatic X-rays, resulting in the emission of photoelectrons whose energies are characteristic of the elements and their chemical/oxidation state, and the intensities of which are reflective of the amount of those elements present within the sampling volume. Photoelectrons are generated within the X-ray penetration depth (typically many microns), but only photoelectrons within the top **5-10 nm** are detected. Detection limits are approximately 0.05 to 1.0 atomic %. Major factors affecting detection limits are the element itself (heavier elements generally have lower detection limits), interferences (which can include other photoelectron peaks and Auger electron peaks from other elements) and background (mainly caused by signal from electrons that have lost energy to the matrix). XPS does not detect H or He. The analysis parameters used for the samples are given in Table 6.

| | |
|---|---|
| **Instrument** | Thermo K-alpha |
| **X-ray source** | Monochromated Alk$_\alpha$1486.6eV |
| **Acceptance Angle** | $\pm$30° |
| **Take-off angle** | 90º |
| **Analysis area** | 400$\mu$m×600$\mu$m |
| **Charge Correction** | C1s 284.8eV (C-C, C-H) |

Table 6. Analysis parameters used for the samples.

Low levels of BN were detected on all surfaces, while the level of BN was found significantly higher on sample #3 (the sample fired with the highest BN content in the propellant). Sample #1 was not expected to have any BN, but since XPS is quite sensitive to boron and nitrogen in the top 5 nm of the surface, it is possible that cross-contamination occurred during the barrel cleaning process, during machining, or during sample handling. The BN content was lowest in Sample #1. The B:N ratio for each sample was summarized in Tables 7-11. Samples #1, #2 and #4 all had very high levels of organic species which may have masked an underlying BN layer. These organic species likely included silicone in addition to S- and Cl-containing species. Several species were observed on all samples which are not normally associated with steel. These included oxides of Al, Ti, Ba and Pb, in addition to Na, K, Ca, Zn and Bi, possibly from the propellant.

All sample surfaces were composed primarily of B, C, N and O, with lower levels of Na, Al, Si, S, Cl, K, Ca, Fe, Zn, Pb and Bi (see Table 7 and Figure 20). While Sample #1 was predominantly Fe on the surface in SEM/EDAX analysis, it should be noted that different “land” circumferential positions were analyzed. Very trace levels of Ti and Ba were detected on some surfaces. Nitrogen was found primarily as BN with lower levels of organic N (see Table 9 and Figure 21), while boron was found as BN (see Figure 22). The level of BN was found significantly higher on sample #3.

Carbon was found primarily as hydrocarbon, with lower levels of carbon-oxygen, carbon-nitrogen and carbon-chlorine functionalities (see Table 8 and Figure 21). Chlorine was found as a combination of organic and inorganic species (see Table 10 and Figure 22). Sulfur was found as a combination of sulfate, sulfide and/or thiol (see Table 11 and Figure 23). Please note that spectral interference from the Bi 4f signal increases the uncertainty in the quantification of S. Silicon was found as $SiO_x$, possibly as silicone and/or silicate (see Figure 24). Aluminum and barium were found as $AlO_x$ and $BaO_x$,

respectively (see Figure 24). Iron was found as a combination of $Fe^{2+}$ and $Fe^{3+}$, likely as $FeO_x$ (see Figure 24). The binding energies of Pb and Ti were associated with $PbO_x$ and $TiO_x$, respectively (see Figure 25). Please note that spectral interference from the Zn 3s signal has increased the uncertainty in the quantification of Pb. The binding energies of Na, K, Ca, Zn and Bi do not shift significantly with different bonding partners; thus, the exact bonding states of these elements were not determined.

Overall, the XPS analysis agrees with previous analysis that Sample #3 contains more residual boron, as expected, since the sample was fired with more boron nitride additive. Sample #1 appears to have more organic residue than detected by SEM/EDAX; however, this sample does have the highest surface iron content, as detected by SEM/EDAX. The ratio of B:N is consistent with boron being predominantly in the form of BN. Other elements on the surface may be from gun powder residue. While the absolute XPS values do not agree with EDAX, it should be noted the analysis depths are quite different (1-2 microns versus 5-10 nanometers) and different circumferential locations were analyzed. The general trends appear to make sense, assuming a small amount of cross-contamination occurred between the samples (i.e., B and Ti detected in all samples).

| | B | C | N | O | Na | Al | Si | S | Cl | K | Ca | Ti | Fe | Zn | Ba | Pb | Bi |
|---|---|---|---|---|---|---|---|---|---|---|---|---|---|---|---|---|---|
| **Sample #1** | 2.6 | 71.5 | 3.3 | 12.8 | 0.4 | 0.4 | 3.1 | 1.6 | 1.5 | 0.6 | 0.2 | <0.1 | 0.4 | 1.0 | 0.1 | 0.1 | 0.2 |
| **Sample #2** | 5.0 | 70.4 | 4.7 | 11.7 | 0.2 | 0.6 | 1.6 | 1.7 | 1.6 | 0.3 | 0.2 | <0.1 | 0.3 | 1.4 | <0.1 | <0.1 | <0.1 |
| **Sample #3** | 22.1 | 37.7 | 18.4 | 14.0 | - | 1.1 | 2.0 | 1.2 | 1.1 | 0.2 | 0.3 | - | 0.2 | 1.6 | <0.1 | 0.1 | <0.1 |
| **Sample #4** | 5.4 | 75.0 | 4.0 | 8.7 | 0.2 | 0.1 | 2.1 | 1.5 | 1.5 | 0.6 | 0.1 | 0.4 | 0.1 | 0.2 | - | <0.1 | <0.1 |

[a] Normalized to 100% of the elements detected. XPS does not detect H or He.
[b] A dash line "-" indicates the element is not detected.
[c] A less than symbol "<" indicates accurate quantification cannot be done due to weak signal intensity.
[d] A question mark "?" indicates species may be present at or near the detection limit of the measurement.

**Table 7: Atomic Concentrations (in mole %)** [a, b, c, d]

| | C-C, C-H | C-O, C-N | C=O, C-$Cl_x$ | O-C=O, C-$Cl_y$ |
|---|---|---|---|---|
| **Sample #1** | 89 | 10 | 1 | <1 |
| **Sample #2** | 89 | 10 | 1 | <1 |
| **Sample #3** | 83 | 13 | 3 | 1 |
| **Sample #4** | 94 | 5 | 1 | <1 |

**Table 8: Carbon Chemical States (in % of Total C[a])**

[a] Values in this table are percentages of the total atomic concentration of the corresponding element shown in Table 9.

| | BN | Organic N | B: N (as BN) | B:N (total N) |
|---|---|---|---|---|
| **Sample #1** | 77 | 23 | 1.00 | 0.77 |
| **Sample #2** | 84 | 16 | 1.26 | 1.07 |
| **Sample #3** | 97 | 3 | 1.24 | 1.20 |
| **Sample #4** | 90 | 10 | 1.49 | 1.34 |

[a] Values in this table are percentages of the total atomic concentration of the corresponding element shown in Table 9.

**Table 9: Nitrogen Chemical States (in % of Total N[a])**

| | Inorganic Cl | Organic Cl |
|---|---|---|
| **Sample #1** | 74 | 26 |
| **Sample #2** | 59 | 41 |
| **Sample #3** | 65 | 35 |
| **Sample #4** | 62 | 38 |

[a] Values in this table are percentages of the total atomic concentration of the corresponding element shown in Table 9.

**Table 10: Chlorine Chemical States (in % of Total Cl[a])**

| | Sulfide, Thiol | Sulfate |
|---|---|---|
| **Sample #1** | 81 | 19 |
| **Sample #2** | 77 | 23 |
| **Sample #3** | 83 | 17 |
| **Sample #4** | 75 | 25 |

[a] Values in this table are percentages of the total atomic concentration of the corresponding element shown in Table 9.

**Table 11: Sulfur Chemical States (in % of Total S[a])**

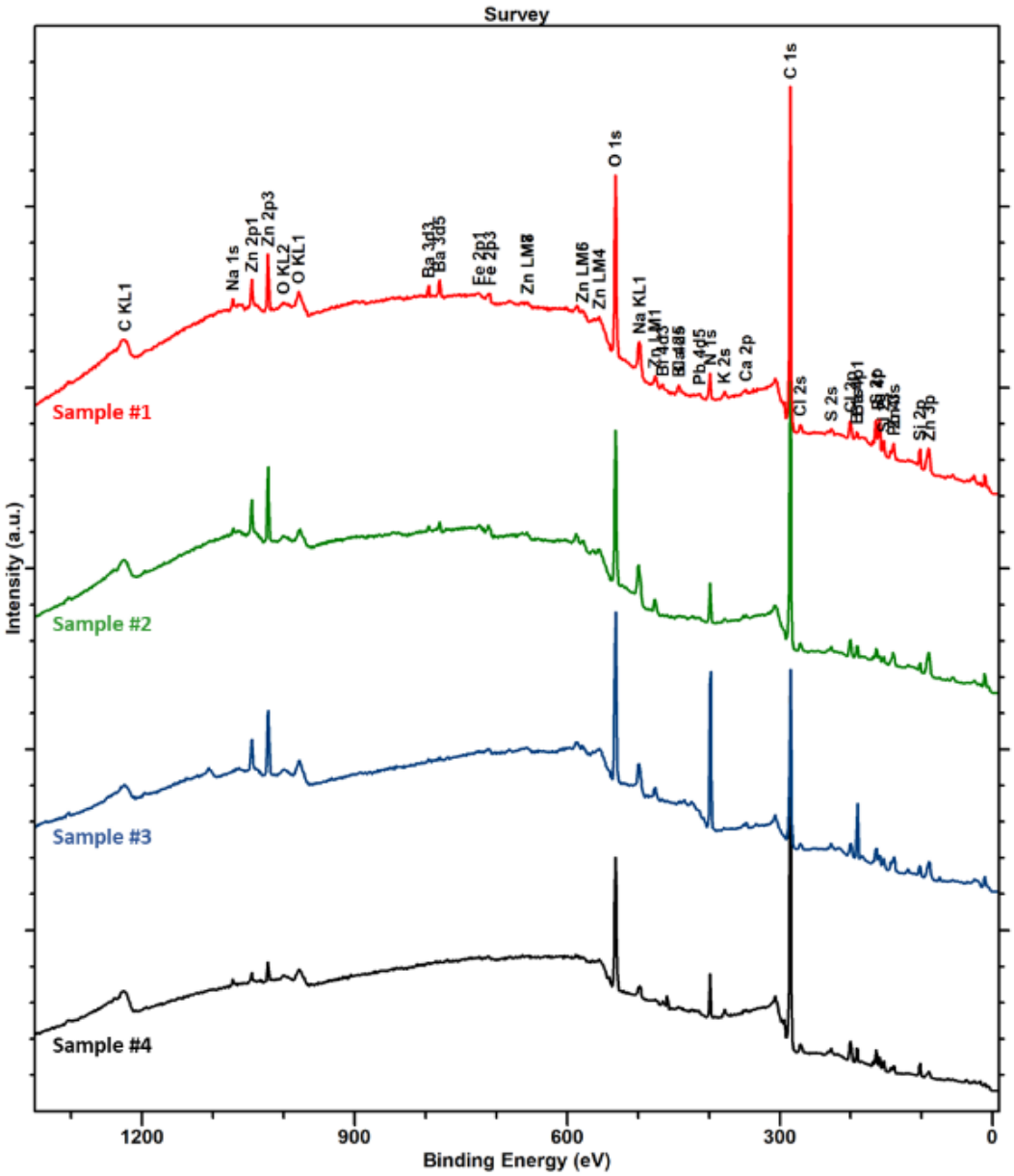


**Figure 20.** XPS survey scan of the samples.

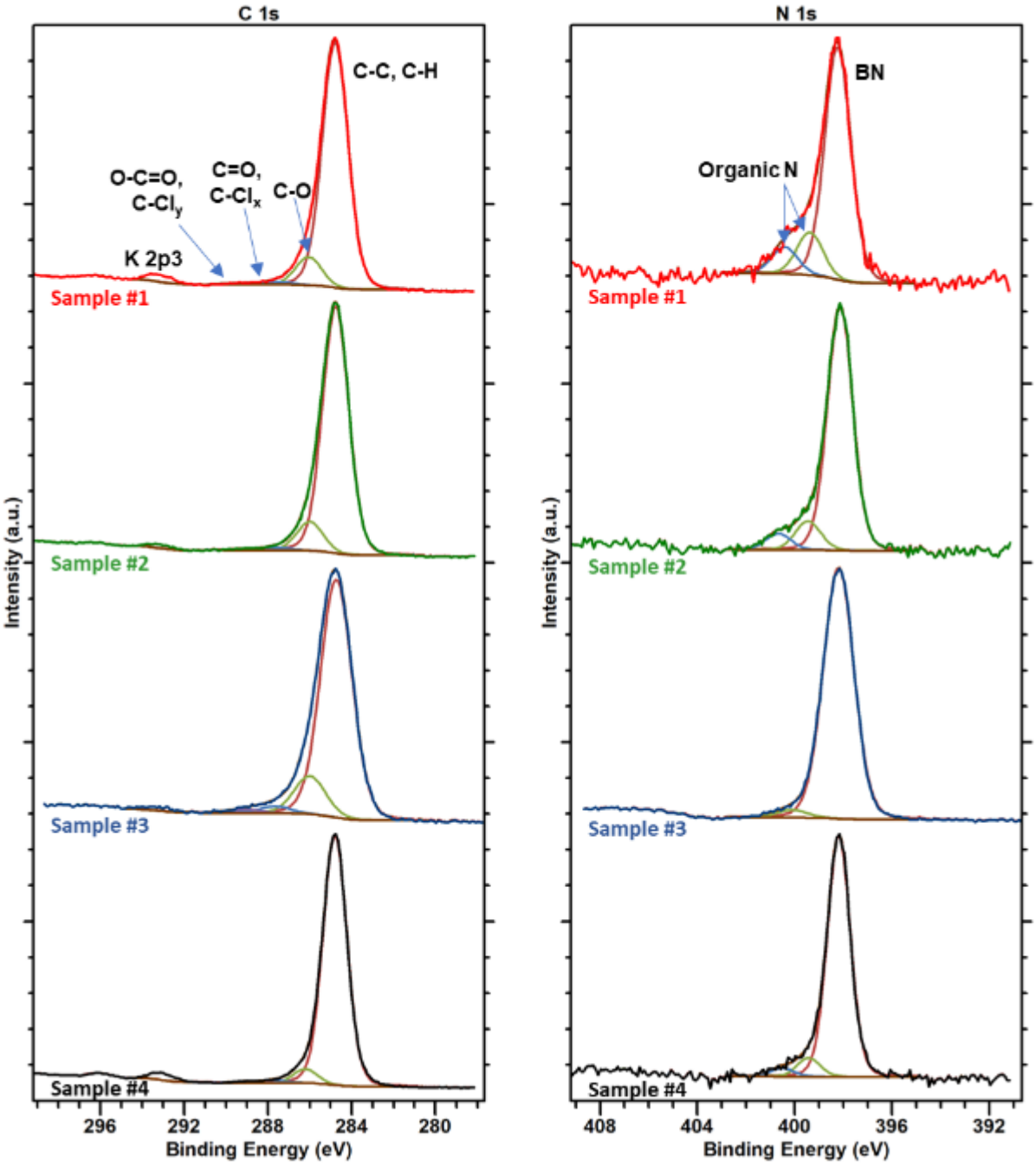


**Figure 21.** XPS analysis of the C and N regions.

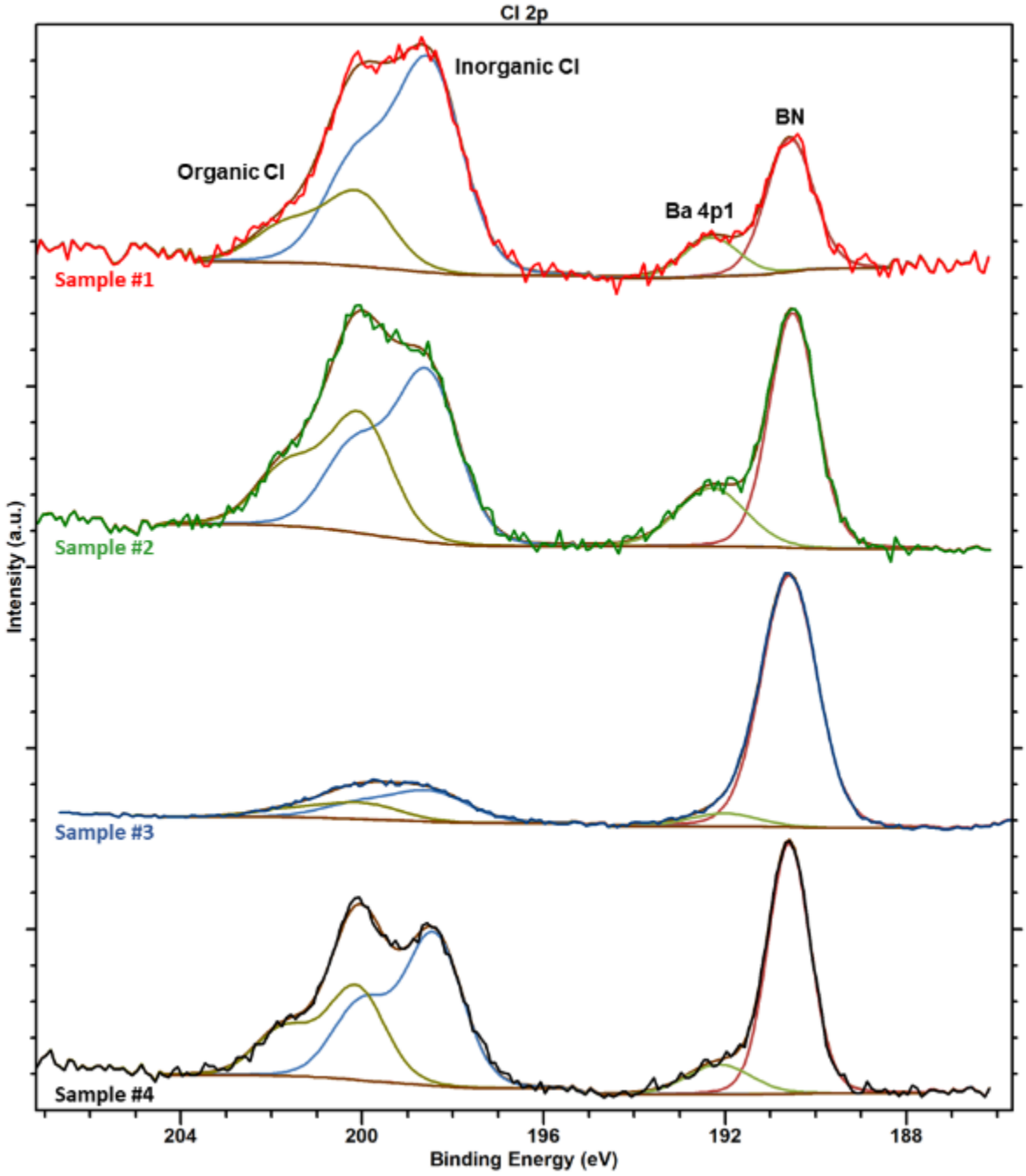


**Figure 22.** XPS analysis of the Cl 2p, Ba, and B regions.

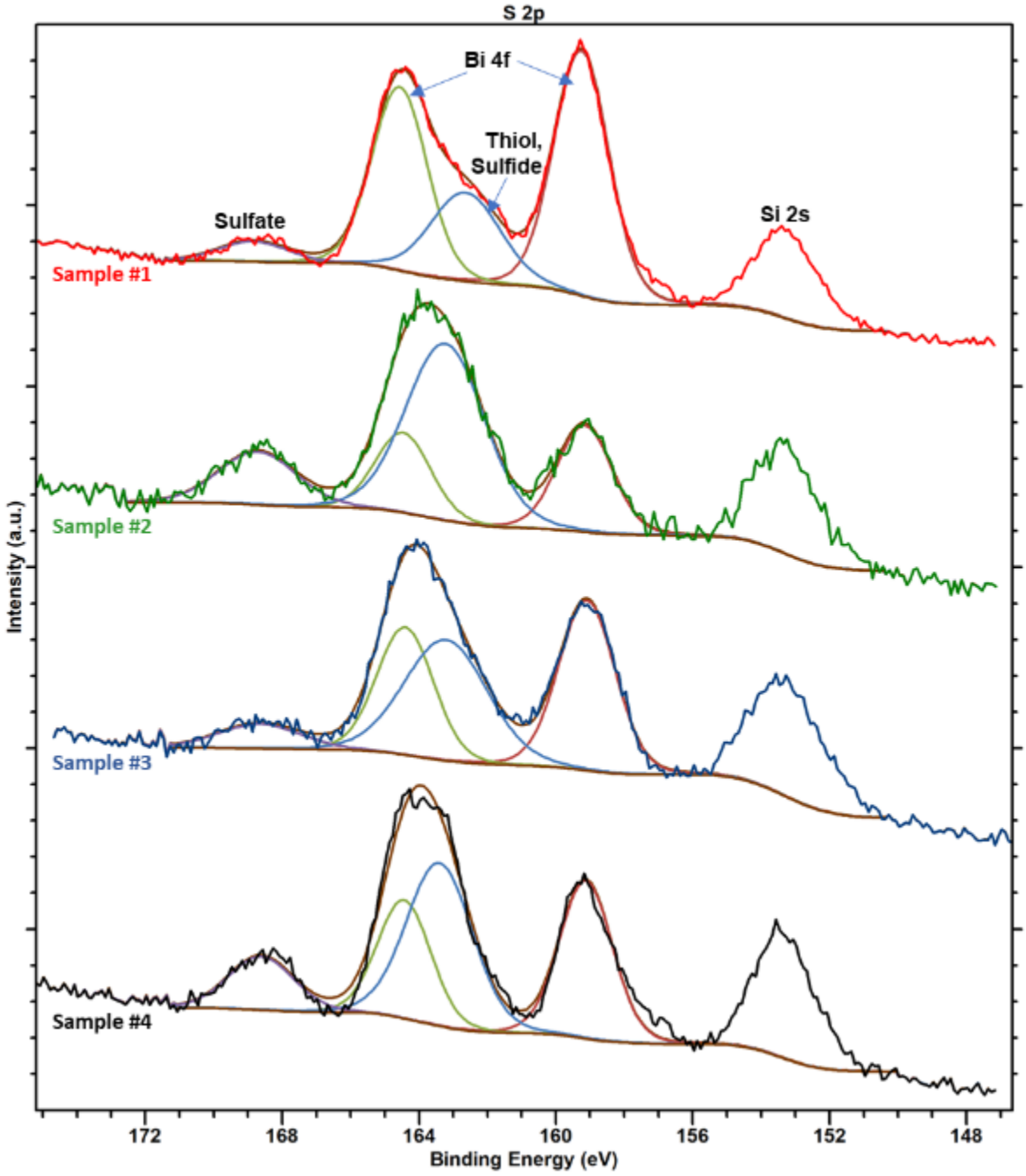


**Figure 23.** XPS analysis of the S 2p, Bi, and Si regions.

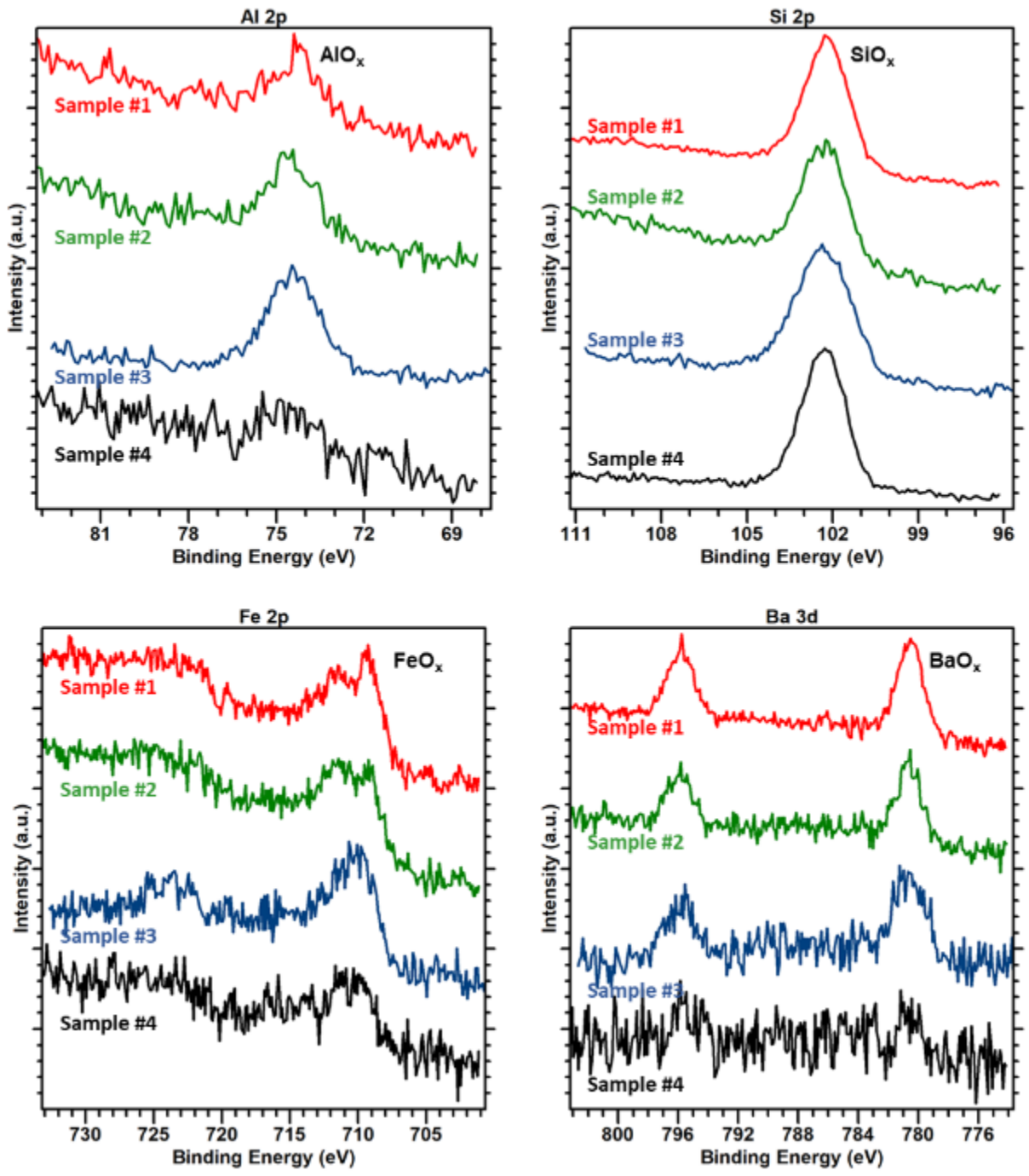


**Figure 24.** XPS analysis of the Al, Si, Fe and Ba regions.

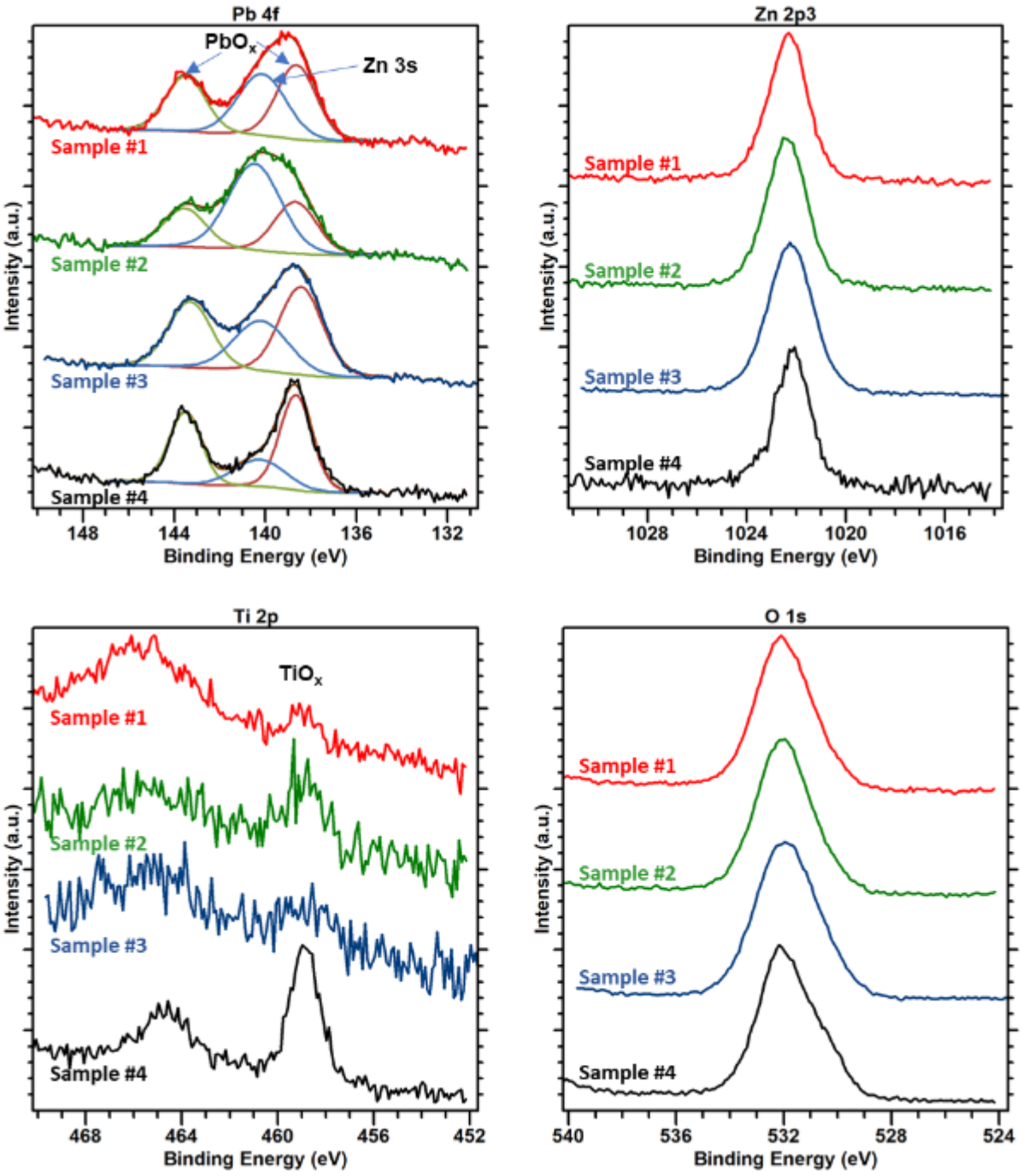


**Figure 25.** XPS analysis of the Pb, Zn, Ti, and O regions.

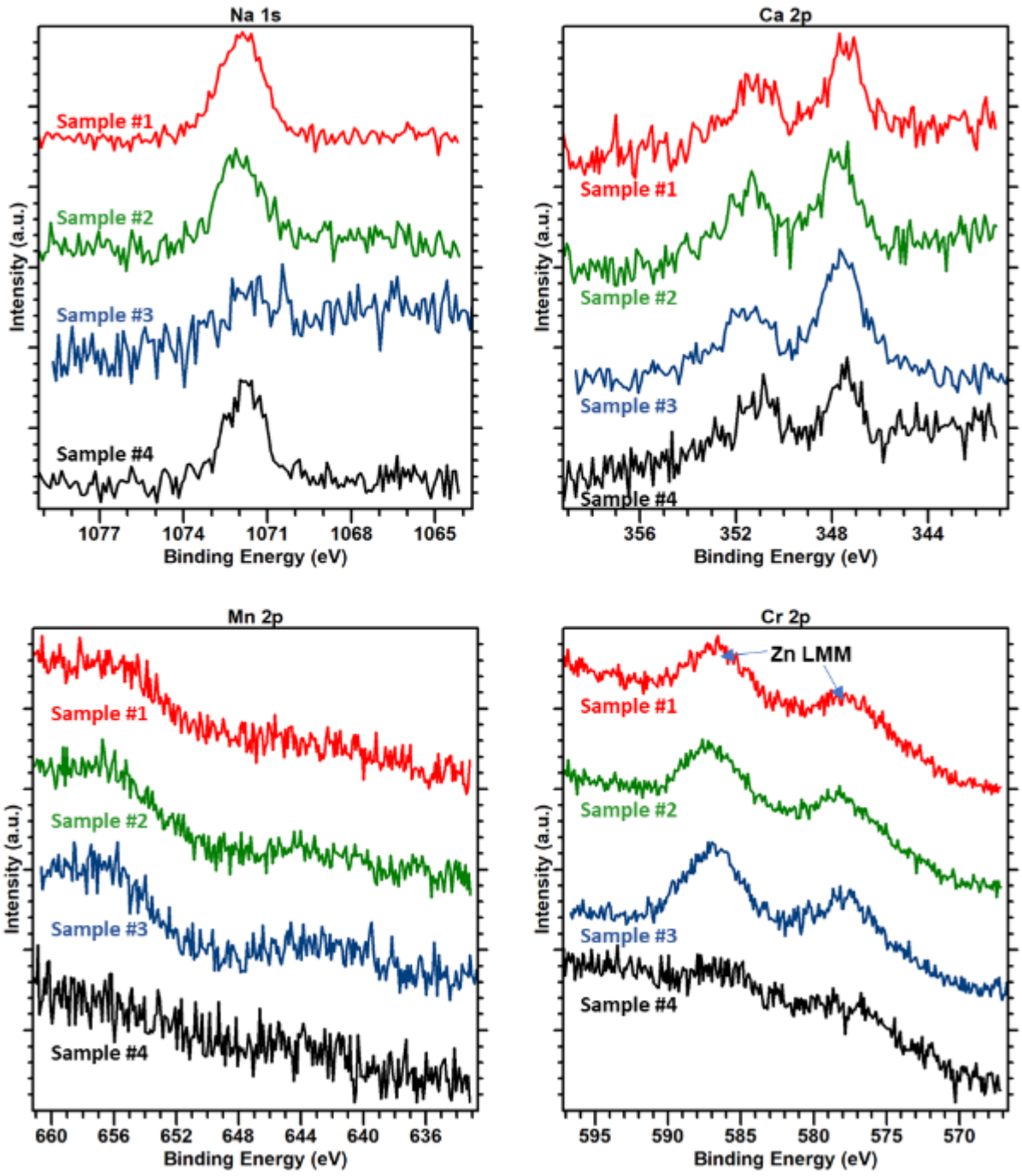


**Figure 26.** XPS analysis of the Na, Ca, Mn, and Cr regions.

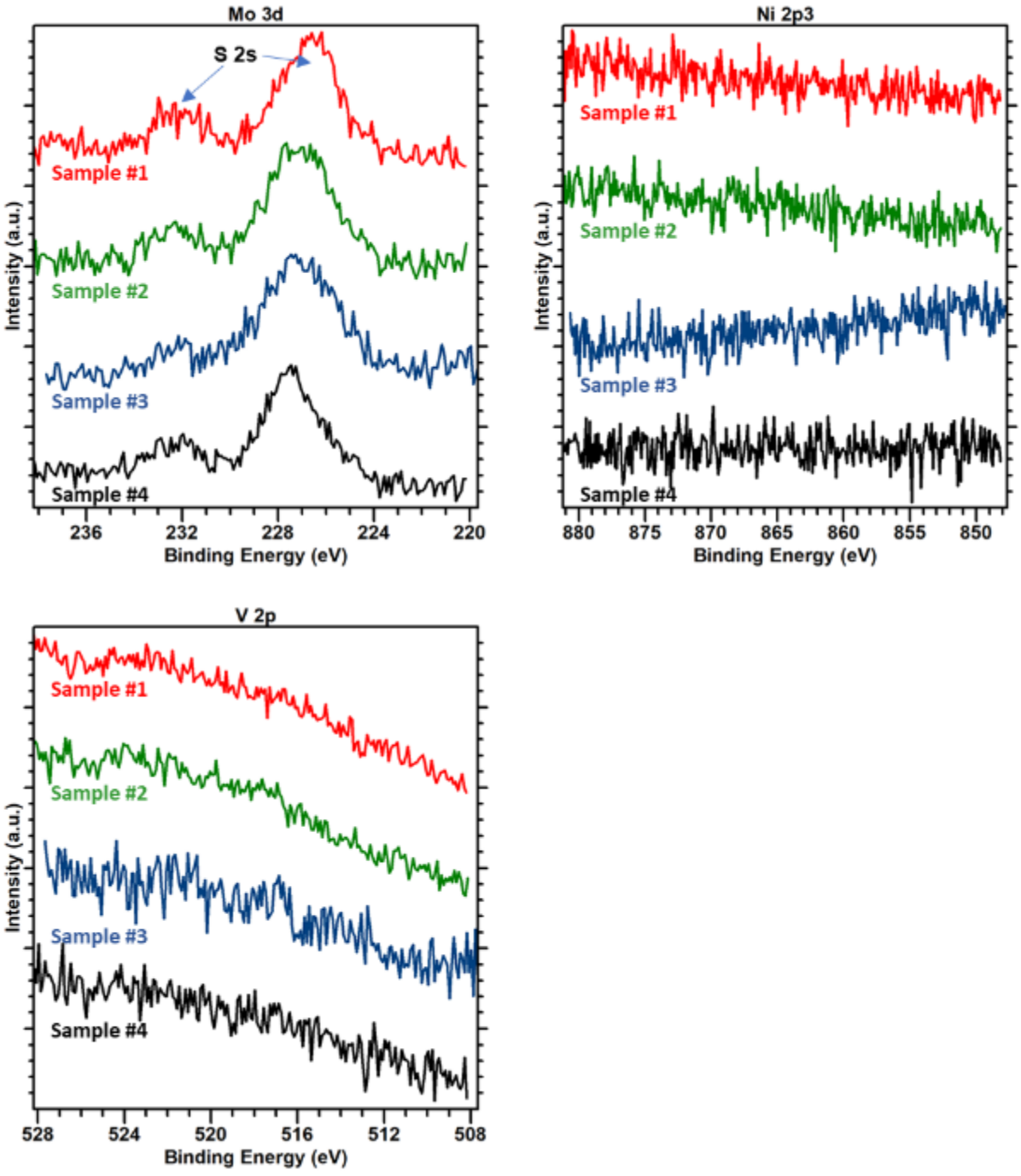


**Figure 27.** XPS analysis of the Ni, Mo, and V regions.

## SUMMARY AJND CONCLUSION

A scalable and economical process for production of BN nano-particles has been developed. These particles were confirmed to be spherical, with an average size less than 200 nm, and can be dispersed in propellants using the conventional solvent approaches. The particles were confirmed to not destabilize nitrocellulose-based propellants, such as the RPD-380, Accurate No. 2, and IMR 4198. To simulate the interaction of BN nano-particles with gun barrels under combustion environments, steel inserts were fired in a closed bomb test chamber in the presence of IMR-4198 propellant compositions with and without the BN additive. Samples fired with BN additive in the propellant showed signs of less oxidation in this testing. XPS showed that boron oxide coated the surface of samples fired with BN additive, and less iron was present on the surface in samples that were less oxidized. SEM and EDAX analysis showed stark differences in surface morphology and composition for samples fired with or without BN additive. Samples fired with BN had a boron oxide surface coating of flat platelets and seemed to lack significant iron oxide (less than 10%). Samples fired without BN were covered with pits, bumps, and octahedral crystals indicative of $Fe_3O_4$. Hardness testing of the insert surfaces was performed to quantify any differences between samples, but the results for these samples were inconclusive.

Further wear and erosion testing was conducted at ARDEC (Benet Labs) using RPD-380 propellant with and without BN. In these tests, the BN additive was demonstrated to reduce wear and erosion by a factor of 2-3 in the limited testing (up to 4 rounds). Post-test characterization at pH Matter found only a small amount of boron remained on the surface after firing and cleaning. However, ppm levels of boron doping can harden steel, and an increased hardness was observed in unhardened steel fired with boron nitride additive. SEM imaging showed less surface crack density in the samples fired with boron nitride. Important considerations for any further tests are an alternate grain form to allow larger bomb loading density, and the corresponding larger amount of propellant necessary for that condition, as well as to support a sufficient number of firings to generate supportable statistical conclusions.

In light of the promising results, further wear and erosion testing of the BN propellant additive was conducted in a sub-scale 25-mm gun test to simulate the conditions of 155 mm artillery during a Phase II Enhancement project. The BN additive appeared to have a positive effect on reducing wear and erosion in the gun tests. All compositions showed reduced erosion versus the baseline material, but samples with high BN or BN with other additives showed the most promising results based on SEM imaging and Moh's hardness testing. Further, the analysis techniques all agreed that the sample fired with more BN had significantly more BN coating and the most well-defined machine grooves after firing. These results appear to agree with previous small-scale tests that demonstrated a 2-3X reduction in wear and erosion for propellants containing BN.

## FUTURE WORK

The results on the Enhancement work bring the technology to a TRL 6. Recommended future work includes further testing of the additive with more-corrosive propellants and full-scale gun tests.

## ACKNOWLEDGEMENT

We would like to acknowledge the Small Business Innovation Research (SBIR) programs managed by the US Department of Defense for their support in funding this program.

## REFERENCES

1.) Sopok, S., US Army Benet Labs, CHARGE-ADDITIVE INDUCED GUN-BORE-RESIDUE DEPOSITION MODEL (155-MM SYSTEM MODEL WITH GUN SOLUTION FOR DEPOSIT/SPIRAL WEAR), JANNAF-CM Apr 2011, JANNAF-CM Dec 2014 update, JANNAF-P Jun 2015 update, JANNAF-PEDCS Dec 2015 update, Marriott Hotel, Salt Lake City, Utah.

2.) Sopok, S. , US Army Benet Labs , GUN-BORE DEPOSIT MODEL FOR SINGLE WEAR ADDITIVE CHARGES (155-MM SYSTEM MODEL WITH CHARGE SOLUTION FOR DEPOSIT/SPIRAL WEAR), JANNAF-PM Apr 2012, JANNAF-CM Dec 2012 update, JANNAF-PM Apr 2013 update, JANNAF-PM Jun 2015 update, Marriott Hotel, Salt Lake City, Utah.
3.) Bracuti, A. J. (1988) Wear-Reducing Additives-Role of the Propellant, in L. Stiefel, ed., Gun Propulsion Technology, Vol. 109 of Progress in Astronautics and Aeronautics, AIAA, Washington DC, United States, chapter 12, pp. 377-411.
4.) Sopok, S., O'Hara, P., Pegl, G., Dunn, S., Coats, D. & Nickerson, G. (1999) Unified
5.) Computer Model for Predicting ´Thermochemical Erosion in Gun Barrels, Journal of Propulsion and Power 15(4), 601–612.
6.) Unified Computer Model for Predicting ´Thermochemical Erosion in Gun Barrels, Journal of Propulsion and Power 15(4), 601–612.
7.) Johnston, I.A., Understanding and Predicting Gun Barrel Erosions, DSTO-TR-1757, August 2005, Edinburg, South Australia, Australia 5111.
8.) Hasenbein, R.G., Wear and Erosion in Large Caliber Gun Barrels, Unclassified Army Report, last accessed June 2011 at: http://www.dtic.mil/cgi-bin/GetTRDoc?Location=U2&doc=GetTRDoc.pdf&AD=ADA440980
9.) Tubb Precision Blended Boron Nitride Bullet Coating Kit, website accessed August 2013 at: http://www.davidtubb.com/boron-nitride-coating-bullets
10.) Calik, A., Duzgun, A., Ekinci, A.E., Karakas, S., Ucar, N., Comparison of hardness and wear behavior of boronized and carburized AISI 8620 steels, Acta Physica Polonica A 116 (2009) p. 1029-1032.
11.) Marucci, M., Lawley, A., Causton, R. and Saritas, S. Effect of small additions of boron on the mechanical properties and hardenability of sintered P/M steels last accessed on 6/17/2011 at: http://www.hoeganaes.com/TechPapersv2/113.pdf
12.) Suwattananont N, Petrova, R., Zunino, J., Schmidt, D., Surface treatment with boron for corrosion protection, Tri-Service Corrosion Conference (2005). Last accessed 6/17/2011 at: https://www.corrdefense.org/Academia%20Government%20and%20Industry/06T041.pdf
13.) Qian, L. and Stone, G.A. A Study of the behavior of boron diffusion in plain carbon steels, Journal of Materials Engineering and Performance 4 (1995) p. 59-62.
14.) Fichtl, W. Boronizing and Its Practical Applications, Materials and Design (1981), p. 276-28